GENETIC MONITORING OF THE RIO GRANDE SILVERY MINNOW: GENETIC STATUS OF WILD AND CAPTIVE STOCKS IN 2022

Annual report FY 2022

Megan J. Osborne, Guilherme Caiero-Dias and Thomas F. Turner
Department of Biology and Museum of Southwestern Biology MSC 03-2020,
University of New Mexico New Mexico, 87131, USA

Agreement: R19AP00025

Submitted to:
Jennifer Bachus and Eric Gonzales
U. S. Bureau of Reclamation-UC-AAO
Albuquerque, New Mexico.
31st October 2022

Table of contents

List of Tables and Figures

EXECUTIVE SUMMARY

Genetic monitoring of the middle Rio Grande population of Rio Grande Silvery Minnow (*Hybognathus amarus*) has been conducted annually from 1999-2012 and 2014-2022. This work includes monitoring stocks that were bred or reared in captivity and released to the Rio Grande in New Mexico. Genetic monitoring of captive stocks commenced in 2002; marking the commencement of the augmentation program. In 2022, genetic monitoring was based on genotyping 339 untagged Rio Grande Silvery Minnow collected from all three occupied reaches of the middle Rio Grande (Table 1 and Table 2), as well as progeny of captive stocks from Southwestern Native Aquatic Resources and Recovery Center (Southwestern ARRC), Albuquerque Biological Park and the Los Lunas Silvery Minnow Refugium (LLSMR). These fish represent the potential breeding population in 2022. We also genotyped broodstocks held at Southwestern ARRC (YC2019, YC2020), Albuquerque Biological Park (YC2019, YC2020, YC2021) and from the LLSMR (YC2021).

Major findings for 2022

(1) Gene diversity and allelic diversity were similar to values recorded in 2021 (Table 3, Figure 1). Observed heterozygosity remained low (also reflected by inflated values of F_{IS}); this means that more individuals had identical alleles at microsatellite loci than in most previous years. Increased homozygosity can be an indication of increased matings between related individual (that share some alleles). At the reach level, diversity measures were all above benchmark values (Figure 2). Allelic diversity and gene diversity were virtually identical between the Angostura and San Acacia reaches. For samples collected from the Isleta reach, allelic diversity and gene diversity were both lower than values recorded in 2021.

(2) In 2022, mitochondrial (mtDNA) haplotype richness (number of haplotypes adjusted to account for differences in sample size between collections) decreased over 2021values while gene diversity increased. However, both diversity metrics remained within the range seen across the time series (Table 3, Figure 3). Across all 2022 samples (including hatchery collections) ten haplotypes were detected including two rare haplotypes (I and V) (Table 3); ten haplotypes were also detected from 2018-2021. Among wild collections in 2022, only nine haplotypes were detected. A single wild-caught individual had haplotype E; which was not detected in last year's wild sample suggesting that this haplotype is rare or absent in the middle Rio Grande population. This haplotype is also present at very low frequencies in the captive stocks. This finding suggests that genetic drift may gradually eroding mitochondrial diversity (and presumably diversity elsewhere in the genome). At the reach level, there is considerable variability in both haplotype richness and diversity between years and reaches.

(3) Genetic effective population size estimates based on changes in allele frequencies from one year to the next (N_{eV}) reveal an increase from 2021 values (Figures 6-8). Specifically, the genetic effective size estimate based on microsatellites was N_{eV}=230-530 for the 2021-2022 comparison compared to N_{eV}=56-69 for 2020-2021 period depending on the estimation method used. Likewise, linkage disequilibrium effective size (which refers to the effective size of the parental population of the sample) also increased (N_{eD}=2301) from values in 2021(N_{eD}=1263). Higher values of N_e in 2021-2022 reflect reduced genetic drift for this period. We also jointly estimated the 'immigration' rate (*m*) from the hatchery to the wild (i.e., riverine population) and the effective size of the total population (wild + augmented). Immigration rates from the hatchery to wild population were variable across the time-series with average estimates of *m* almost doubling for the 2012-

2022 period compared the decade preceding the 2012-2014 population bottleneck (2002-2012: $\overline{m}$ =0.166; 2012-2022: $\overline{m}$=0.29). Across the time-series, MLNe estimates that included input of hatchery-reared individuals were smaller (typically half) than wild-only estimates. This result shows that the input of hatchery fish acts as an additional source of genetic drift. The 2021-2022 sample MLNe (wild + hatchery) estimate was 243; an increase from the previous temporal sample.

(4) To augment the wild population, ~204,000 fish were released to the Middle Rio Grande in November/December 2021. We genotyped representatives from three captive lots released to the Middle Rio Grande, including one lot from each hatchery facility (Southwestern ARRC, Albuquerque BioPark and LLSMR). Pooled hatchery samples released to the middle Rio Grande had levels of genetic diversity measured across microsatellite loci that were very similar to the 'wild' population in 2022 with the exception of allelic diversity which was reduced in the captive stocks (Table 3). Haplotype diversity was lower and fewer haplotypes were detected compared to the wild population sampled in 2022 across released pooled hatchery stocks (Table 3). The fewest haplotypes and lowest haplotype diversity were seen in the fish released from the Albuquerque BioPark and estimates of the N_{eD} were also low for this stock and as well as for individuals released from LLSMR.

(5) Broodstocks from Southwestern ARRC, Albuquerque BioPark and the LLSMR were also genotyped in 2022. These samples represent the 2019-2020 year classes (YC) held at Southwestern ARRC as well as the 2019, 2020 and 2021 year classes held at the Albuquerque BioPark, and 2020 and 2021 year classes from the LLSMR. Genetic diversity based on microsatellites and mtDNA of these broodstocks were within the range seen in the wild population. Across all broodstock samples, 10 haplotypes were detected, five haplotypes were common while the others were rare. Finite genetic effective size estimated using the linkage disequilibrium method ranged from 500 (2022-SNARRC-BS-YC19) to 4,933(LLSMR-YC20) across facilities (Table 3). This estimate pertains to effective population size of the generation the produced the current sample. Genetic diversity in the refugial broodstocks is largely dependent upon the strength of the year class from which it was sourced.

INTRODUCTION

Genetic monitoring is defined as a collection of two or more temporally spaced genetic samples from the same population (Schwartz et al. 2007). Such studies typically employ neutral genetic markers and occasionally maternally inherited mtDNA, to track changes in standard genetic diversity metrics (gene diversity [H_E], heterozygosity [H_O], allelic richness [A_R] and genetic effective population size [N_e]) over a contemporary time series (see glossary). It is widely recognized that erosion of genetic diversity increases a species' vulnerability to decline through lowered fitness (e.g., associated with inbreeding depression) that can ultimately accelerate the path to extinction for imperiled species. This is the rationale for tracking these metrics of diversity across time (e.g., Frankham 2005). The time scale of genetic monitoring varies considerably among studies from sampling over only a few years to the use of archival samples for a monitoring program that may span decades. In studies that encompass multiple decades, sampling is rarely conducted on an annual basis so linking changes in diversity metrics with specific environmental or management actions may not be plausible. In fish, genetic monitoring to date has been confined largely to marine species and freshwater salmonids. The genetic data that we have collected for Rio Grande Silvery

Minnow spans a 34-year period (1987, 1999-2012, 2015-2021) and represents one of the longest genetic monitoring time series for a non-salmonid freshwater fish.

For genetic monitoring programs, empirical measurements of diversity and genetic effective size are typically obtained from neutrally-evolving microsatellite loci. Microsatellites are short tandemly repeating DNA sequences that are found throughout the genome of most species (reviewed in Dowling et al. 1996). They are bi-parentally inherited and are highly polymorphic among individuals (which is particularly important for endangered species that may have limited genetic diversity) and hence are the most widely used genetic markers in molecular ecology and conservation genetics studies. MtDNA is a haploid marker (i.e., individuals only have one copy as opposed to two copies for microsatellites), so progeny inherit a single mtDNA molecule from the female parent only. Due to differences in how nuclear DNA and mtDNA are inherited, they provide complementary approaches to monitoring genetic diversity.

The Rio Grande Silvery Minnow is a small-bodied (<90 mm standard length), short-lived (in the spring the vast majority of fish are age-1; Horwitz et al. 2018) cyprinid. This species was historically widely distributed in the Rio Grande from northern New Mexico to the Gulf of Mexico, and in the Pecos River from northern New Mexico to the confluence of the Rio Grande in Texas (Pflieger 1980). Habitat changes associated with river fragmentation caused by water storage dams and diversion structures and changes to the natural hydrograph have resulted in significant range contraction. The interaction of these factors with species life-history causes changes in population density that can span several orders of magnitude from one year to the next (Dudley et al. 2021). Over the past 20-years, periodic droughts and resulting channel dewatering have caused recruitment failure in some years and periodic population collapse (Archdeacon et al. 2020a). Today a remnant population persists in the highly fragmented and regulated Rio Grande in New Mexico. This 280-km river segment represents less than 5% of the historical range of the species and extends from downstream of Cochiti Dam to Elephant Butte Reservoir. This stretch of river is bisected by three water diversion structures that define distinct river reaches (from north to south: Angostura, Isleta, and San Acacia). Rio Grande Silvery Minnow was listed under the Endangered Species Act in 1994 (U.S. Fish and Wildlife Service 1994). This species is now intensively managed including a captive breeding program and annual augmentation of the Rio Grande population that has been in place since 2003 (U.S. Fish and Wildlife Service 2018).

The Rio Grande Silvery Minnow population is sampled annually throughout its current range and the trajectory of genetic diversity (including allelic richness, heterozygosity, and genetic effective population size) is measured using nine microsatellite loci and a mtDNA gene. The temporal component and sampling strategy provide the framework necessary to examine impacts of changes in abundance, management actions and environmental conditions on genetic diversity at these loci. Negative genetic impacts to a population can occur over relatively short time periods for fishes characterized by a short lifespan (the population is dominated by age-1 fish in the spring; Horwitz et al. 2018) and in which dramatic changes in abundance occur from year to year. While repeated augmentation buffers the population against dramatic population declines, there are also potential genetic consequences of this strategy. As such, genetic monitoring is a crucial component to management of Rio Grande Silvery Minnow. Here we report on the genetic status of the population in 2022 and compare these results to previous years.

MATERIALS AND METHODS

Sampling- Rio Grande population

Throughout this study, we use the term 'wild' to refer to unmarked fish sampled directly from the Rio Grande, as opposed to individuals tagged with a Visible Implant Elastomer (VIE) tag to indicate that they were reared in a hatchery and used to supplement the Rio Grande Silvery Minnow population. We use the term 'wild caught hatchery' (WCH) to refer to individuals with a VIE tag. 'Wild' fish may have parents that were wild or bred/reared in captivity, but were hatched in the Rio Grande. In 2021, only a fraction of released fish were tagged so collections likely consist of both wild-born and hatchery released individuals. Unmarked Rio Grande Silvery minnow were collected between December 16th 2021 and March 8th 2022 (n=339); these are assumed to represent the potential breeding population in 2022. These samples add to the data collected from wild Rio Grande Silvery Minnow sampled from the middle Rio Grande annually from 1999 to 2012 and 2014-2021 (between November and April- just prior to reproduction) as well as 43 individuals used in a previous allozyme study of *Hybognathus* and stored in the Museum of Southwestern Biology Division of Genomic Resources (Cook et al. 1992 - referred to as 1987 sample). The distinction is made between 'wild' and WCH fish for this reason and because population monitoring tracks 'wild' fish separately from hatchery released fish. Collections were made throughout the current distribution (i.e., from Cochiti reservoir to Elephant Butte reservoir in New Mexico) of Rio Grande Silvery Minnow, with the exception of the Cochiti reach because the species is rare or absent in that area (Bestgen and Platania 1991). In 2022, untagged fish were collected from all occupied river reaches by seining a variety of habitats in the Angostura (n=159), Isleta (n=51) and San Acacia (n=131) reaches (Table 1, Table 2). Rio Grande silvery minnow were uncommon in the Isleta reach. Fish were anesthetized in river water treated with MS-222 (Tricaine methane sulfonate 200 mg/L river water) at the site of capture. A piece of caudal fin was removed from each individual. Fin clips were preserved in 95% ethanol.

Sampling- Captive lots and Broodstock

Fin clips representing fish released in fall 2021 from Southwestern ARRC (n=100), Albuquerque BioPark (n=50) and LLSMR (n=99) were genotyped. We also genotyped broodstocks held at Southwestern ARRC (2019 n=95, 2020 n=95), Albuquerque Biological Park (YC19 n=95, YC20 n=190, YC21 n=285) and the LLSMR (YC 2020 n=94).

Table 1. Sample sizes and collection localities of untagged Rio Grande Silvery Minnow by river reach for samples collected during 2022 genetic monitoring. Only a fraction of fish were tagged prior to release so sampled fish are likely a mix of wild-produced and augmented individuals.

Angostura	
Montano Bridge Crossing	50
Central Avenue bridge crossing (US HWY 66)	62
Avenida Cesar Chavez Bridge Crossing	47
Isleta	
Rio Grande downstream of Hwy6 Bridge crossing	36
Rio Grande at 346 bridge crossing	14
San Acacia	
Escondida	32
Ca. 1.5 mi downstream of San Acacia Diversion Dam	51
San Marcial Railroad crossing	47
Grand Total	339

Table 2. All 'wild' samples collected from the middle Rio Grande by river reach for 1987, 1999-2012 and 2014-2022.

*Genetic analysis was not conducted in 2014 due to the small number of samples collected.

Year	Angostura	Isleta	San Acacia	Total
1987	15	-	28	43
1999	-	-	46	46
2000	-	-	194	194
2001	-	65	63	128
2002	67	121	201	389
2003	71	65	33	169
2004	141	15	6	162
2005	190	109	95	394
2006	95	143	145	383
2007	48	128	42	218
2008	165	191	123	479
2009	175	153	150	478
2010	149	146	151	446
2011	71	148	140	359
2012	147	215	154	516
2013	-	-	-	-
2014*	5	3	4	12
2015	75	33	35	143
2016	171	121	128	420
2017	159	156	154	469
2018	152	148	143	443
2019	73	10	54	137
2020	148	127	151	426
2021	118	60	61	239
2022	159	50	130	339

Molecular methods- microsatellites

Total nucleic acids, including genomic and mitochondrial DNA were extracted from air-dried fin clips using proteinase-K digestion and organic extraction methods (Hillis et al. 1996). Individuals were genotyped at nine microsatellite loci: *Lco1*, *Lco3*, *Lco6*, *Lco7*, *Lco8* (Turner et al. 2004); *Ca6* and *Ca8* (Dimsoski et al. 2000); and *Ppro118* and *Ppro126* (Bessert and Orti 2003). The following pairs of loci were amplified through multiplex PCR: *Lco1*/*Ca6* and *Lco6*/*Lco7* (1X PCR buffer, 3 mM $MgCl_2$, 125 micromol [μM] deoxyribonucleotide triphosphates [dNTPs], 0.40-0.50 μM each primer, 0.375 units *Taq* polymerase); *Lco3* and *Lco8* (1X PCR buffer, 2 mM $MgCl_2$, 0.8 mM dNTPs, 0.40-0.50 μM each primer, 0.375 units *Taq*); and *Ppro 118*/*Ppro126* (1X PCR buffer, 3 mM $MgCl_2$, 0.8 mM dNTPs, 0.40-0.50 μM each primer, 0.375 units *Taq*). *Ca8* was amplified alone (1X PCR buffer, 3 mM $MgCl_2$, 0.8 mM dNTPs, 0.50μM each primer, 0.375 units *Taq* polymerase). PCR cycling conditions for all loci were as follows: one denaturation cycle of 92°C for 2 min followed by 30 cycles of 90 °C for 20s, 50°C for 20 s, 72°C for 30s. Cycling conditions for *Ppro 118*/*Ppro126* were as follows: one denaturation cycle of 92°C for 2 min followed by 30 cycles of 90 °C for 20s, 60°C for 20 s, 72°C for 30s. Primer concentrations in multiplex reactions were optimized by locus to ensure equal amplification each microsatellite. Fragment size analysis on an ABI 3130 automated capillary sequencer was performed by combining 1 μl of PCR product with 10 μl of formamide and 0.4 μl of HD400 size standard and denatured at 93°C for 5 minutes. Genotype data were scored in GENEMAPPER Version 4.0 (Applied Biosystems).

MtDNA- ND4

A 295-base pair (bp) fragment of the mtDNA ND4 gene was amplified from each individual in a 10 μL reaction containing 1 μL template DNA, 1 μL 10× reaction buffer, 2 mM $MgCl_2$, 0.8 μM dNTPs, 0.5 μM forward (5'- GAC CGT CTG CAA AAC CTT AA- 3') and reverse primer (5'- GGG GAT GAG AGT GGC TTC AA – 3'), and 0.375 units *Taq*. PCR conditions were 90° C initial denaturation for 2 minutes followed by 30 cycles of 90° C for 30 seconds, 50° C for 30 seconds, and 72◦ C for 30 seconds. Sequence data was obtained for all individuals by direct sanger sequencing (Big Dye vers. 1.1) according to the manufacturer's instructions and using an ABI 3130 DNA Sequencer.

Statistical analysis

GENEPOP'007 (Rousett 2008) was used to test for departures from Hardy-Weinberg equilibrium (HWE), using the procedure of Guo and Thompson (1992) and to perform global tests for linkage disequilibrium for all pairs of loci in each collection. Sequential Bonferroni correction (Rice 1989) was applied to account for inflated Type-1 error rates associated with multiple simultaneous tests. In some cases, sample sizes differed between collections, particularly between some samples collected early in the study and more recent collections. The number of alleles and heterozygosity are dependent on sample size, so we used a resampling approach to correct for sample size effects on diversity measures and make them more comparable across collections. In short, we randomly sampled each collection without replacement using the minimum sample size across all years (n = 43 in 1987). Microsatellite diversity estimates (corrected number of alleles [N_{AC}], Nei's (Nei 1987) gene diversity [H_{EC}] and heterozygosity [observed proportion of heterozygotes] [H_{OC}]) were then calculated for the random sample and the process repeated for 1000 iterations. Corrected diversity estimates are calculated as the mean estimate across all iterations. This analysis was conducted in the R statistical package (www.r-project.org). This resampling technique was also used for comparisons among collections obtained across years and river reaches, we repeated the resampling procedure for microsatellite data with diversity measures based on n=15 (1987, San Acacia) and excluding the smallest samples (2004

San Acacia; Isleta 2019). For each microsatellite locus and population, inbreeding coefficients (F_{IS}) were obtained using the R statistical package *hierfstat* vers. 0.5-7 (Goudet and Jombart 2015, 2020).

Mitochondrial diversity was characterized by number of haplotypes (N_h), haplotype diversity (*h*), and haplotype richness (H_R). These metrics are roughly equivalent to the number of alleles, gene diversity (H_{EC}), allelic diversity (N_{AC}) averaged across microsatellite loci. Haplotype richness (H_R) (Petit et al. 1998) was obtained using the R package *hierfstat* vers. 0.5-7 (Goudet and Jombart 2020). Haplotype diversity (*h*) is a measure of the uniqueness of a haplotype in a population. Values of *h* range from zero (all individuals have the same haplotype) to one (all individuals have a different haplotype). The calculation of *h* is based on the sample size and the frequency of each haplotype in the population.

To place levels of diversity across years in context of overall genetic diversity of the species and to develop a biologically relevant benchmark for assessing levels of diversity within samples, we used an additional resampling technique. All 'wild' fish were pooled into one large population (n = 7,016) from which we iteratively took samples (n = 43 by year; n=15 by reach benchmarks) to estimate diversity statistics. Our primary interest is maintaining genetic diversity, hence we estimated a one-tailed lower 95% confidence intervals that corresponds to the upper 95% of the resampled distribution (i.e., 9500 of 10000 iterations). Thus, the distribution contained within this confidence interval corresponds to the null hypothesis of no loss of diversity.

F-statistics

Weir and Cockerham's (1984) *F*-statistics (microsatellites) and *Φ*-statistics (mtDNA) were calculated using Arlequin ver. 3.11 (Excoffier et al. 2005), respectively. Hierarchical analysis of molecular variance (AMOVA) was used to test whether a significant proportion of genetic variance was partitioned into components attributable to differences among 'wild', captive-spawned, and broodstock fish (F_{CT}, Φ_{CT}), among samples within these three groups sampled in 2022 (F_{SC}, Φ_{SC}) and among all samples (F_{ST}, Φ_{ST}). P-values for all statistics were generated using bootstrapping (9999 permutations).

Temporal genetic structure was evaluated with discriminant analysis of principle components (DAPC), that summarizes genotypes in principle components (PCs) which are used to construct linear functions that maximize among group variation while minimizing within group variation, using the R package *adegenet* v. 1.3-1 (Jombart and Ahmed 2011). Prior to DAPC we replaced missing data within each group using the Breiman's regression random forest algorithm (Breiman 2001) implemented in R package randomForest v. 4.6–14 (Liaw and Wiener 2002). Values of missing data in the microsatellite (2% total MD) dataset was predicted from 500 independently constructed regression trees and 50 bootstrap iterations with default bootstrap sample size. This was preferred over the default "mean method" (i.e., missing genotypes are replaced by the average estimated across the dataset) implemented in *adegenet*, to ensure that we did not artificially increase similarity of allele frequencies across years. A first DAPC was performed using years as groups, without scaling allele frequencies, retaining all PCs and DAs, and keeping other options as default. The *a-score* method was used to select the optimal number of PCs retained for final DAPC. This was performed using the maximum number of PCs found with first DAPC, all DAs with the other options set as default. The final DAPC was performed using the optimal number of PCs, two DAs, and retaining the other default options.

Estimation of genetic population effective size and geneflow

Variance effective size (N_{eV}) and 95% confidence intervals (CIs) were estimated from annual changes in microsatellite allele frequencies across annual samples, using the temporal methods of Nei and Tajima (1981) and Jorde and Ryman (2007), implemented in NEESTIMATOR vers 2.1 (Do et al. 2014). Highly polymorphic loci with many rare alleles, typical of microsatellites, can result in biased estimates of N_{eV} (Hedrick 1999; Turner et al. 2001). To minimize this bias, we used the P_{CRIT} value 0.02 to exclude low frequency alleles. Rio Grande Silvery Minnow were sampled under Plan I (prior to reproduction, with replacement) for all methods. The parametric method was used to calculate 95% confidence intervals. Multiple temporal methods are used to calculated N_{eV} to ensure consistency across estimators. We also used the program MLNe v. 1.0 (Wang and Whitlock 2003) to estimate N_e (N_{eW}).

Genetic drift associated with 'immigration' can bias genetic effective population size estimates. Under these circumstances, Wang and Whitlock (2003) and Gilbert and Whitlock (2015) found that the likelihood estimators implemented in the program MLNe provided the most accurate N_e estimates. For this reason, we jointly estimated the average immigration rate (*m*) and variance effective size of the total population (referred to as N_{eT}) using the likelihood method implemented in MLNe. We set prior max N_e as 10,000. Annual source populations were a representative sample of individuals released from the hatcheries and likely contributing to the breeding population in a given year. For example, for N_e calculated between 2004 and 2005, fish released in fall 2004 were included as the source population for '*immigrants*'. MLNe estimates of only the wild samples are refered to as N_{eW}.

Variance effective size was also estimated for the female portion of the population using mtDNA haplotype frequencies. To distinguish between variance effective size based on microsatellite data (N_{eV}) we use the designation N_{ef} to represent mtDNA variance effective size. N_{ef} was estimated with the pseudo-maximum-likelihood (MLNe) method (Wang 2001). It is useful to estimate genetic effective size from mtDNA data because it provides information pertaining to the female portion of the population. For example, when very low estimates of N_{ef} are obtained it implies that relatively few females are making a genetic contribution to the population.

We equated the number of years separating a pair of samples with the number of generations elapsed between samples because Rio Grande Silvery Minnow have essentially non-overlapping generations (based on unpublished population monitoring data of R. K. Dudley and S. P. Platania). However, to account for small but known deviation from the discrete generation model (G = 1.27), we corrected consecutive estimates of N_{eV} (and N_{eW}, N_{eT}) and N_{ef} for overlapping generations (Turner et al. 2006; Osborne et al. 2010), using the analytical method of Jorde and Ryman (1995, 1996). In addition to consecutive pairwise estimates, we also present comparisons between the 1987 and 1999 samples to provide historical context for the contemporary estimates. As these samples (1987-1999) were collected more than 3-5 generations apart, the drift signal should be sufficiently large relative to sampling biases associated with age-structure such that correction for overlapping generations is unnecessary (Waples and Yokota 2007).

We used the linkage disequilibrium method (Hill 1981) that only requires a single temporal sample to estimate the linkage disequilibrium effective size (N_{eD}). Annual N_{eD} was estimated from microsatellite DNA data separately for 'wild', captive-spawned stocks, and broodstock samples using the updated version of the program NEESTIMATOR vers. 2.1 (Do et al. 2014). Single sample N_e methods (such as those provided by

N_{eD}) yield an estimate of the effective number of parents that produced the progeny from which the sample is drawn, and most closely approximates the inbreeding effective size, N_{eI} (Laurie-Ahlberg and Weir 1979; Waples 2005). Confidence intervals were determined using the jack-knife procedure implemented in NeEstimator.

RESULTS

Microsatellites- genetic diversity

Characterization of microsatellite genotypes from the 2022 samples (wild-collected and hatchery) revealed two loci (*Ca6* and *Ppro126*) as the least variable, each with 8 alleles detected across samples. Locus *Ppro118* was the most variable with 63 alleles followed by *Lco1* with 43 alleles detected across collections. In 2022, tests for deviations from Hardy-Weinberg Proportions were significant for 36% of locus-by-population combinations (45/126) following sequential Bonferroni correction for multiple comparisons. The majority of significant departures occurred at four loci (*Lco7*, *Lco8*, *Ppro118*). Analysis by MICRO-CHECKER (Van Oosterhout et al. 2004) found that presence of null alleles was the most likely explanation for an excess of homozygous individuals. Four loci (*Lco3*, *Lco6*, *Ca6, Ppro126*) conformed to Hardy-Weinberg expectations in all collections, *Lco3, Lco1* and *Ca8* departed from expectations in one, four and six collections respectively. Across all collections, significant tests for genotypic disequilibrium occurred in seven of 504 comparisons following sequential Bonferroni correction.

Genetic diversity statistics based on microsatellite data of wild-collected Rio Grande Silvery Minnow sampled in 2022 (H_{EC}= 0.817, H_{OC} = 0.701, and N_{AC}= 14.7) were within the range of values observed since monitoring began (Table 3, Fig. 1). The lowest number of alleles and heterozygosity were observed in the 1987 sample (N_{AC} = 13.8, H_{OC} = 0.676) and lowest gene diversity (H_{EC}= 0.782) was recorded in 2002; prior to the commencement of population augmentation. We used a resampling approach of all 'wild' fish collected between 1987-2022 to determine diversity benchmarks based on microsatellites that correspond to annual diversity estimates based on the minimum annual sample size (n = 43 [year], n=15 [reach]). Diversity benchmarks at the annual level were: H_{EC} = 0.802, H_{OC} = 0.676, and N_{AC}= 14.8 and at the reach level were: H_{EC} = 0.767, H_{OC}= 0.642, and N_{AC}= 9.7 (Fig. 1). Gene diversity and H_{OC} for 2022 wild-collected fish exceeded these benchmarks at both annual and reach level. From analysis of microsatellite data by river reach for the 2022 sample H_{EC} and H_{OC} exceeded the minimum benchmark values. Allelic diversity for individuals collected from the Isleta reach was identical to the benchmark values (N_{AC}=9.7) while values for this metric were higher in both the Angostura and San Acacia reaches.

Gene diversity, H_{OC} and N_{AC} for pooled captive lots released to the Rio Grande in 2021 were greater than the 95% CI genetic diversity benchmark (Table 3). In the refugial broodstocks sampled in 2021-2022 from the three facilities, H_{EC} exceeded the benchmark values and this was also the case for H_{OC} with a single exception (22LLSMR-Bs-WC20) (Table 3). Allelic diversity fell below the benchmark values in most refugial captive stock with the exception of 2022-LLSMR-Bs-YC20, 2022-ABP-BS2 (ABP20-Wild-San Acacia) and 2022-ABP-BS3 (ABP20-Wild-San Acacia).

Table 3. Diversity statistics for microsatellites and mtDNA.

N is sample size, N_{AC} is average number of alleles across loci, H_{EC} is Nei's gene diversity, H_{OC} is observed heterozygosity, F_{IS} is inbreeding co-efficient, N_h is number of haplotypes, *h* is haplotype diversity, and H_R is haplotype richness. Linkage disequilibrium estimates of effective size, N_{eD}, are also given (95% confidence intervals are denoted as lci and uci). Genetic monitoring was not conducted in 2013. Values from 2022 monitoring year are in bold for emphasis; Wild caught hatchery fish (WCH) were included in genetic monitoring beginning 2014.

	Microsatellites								mtDNA			
Wild-MRG	**N**	**N_{AC}**	**H_{EC}**	**H_{OC}**	**F_{IS}**	**N_{eD}**	**lci**	**uci**	**N**	**N_h**	**h**	**H_R**
1987	43	13.8	0.786	0.71	0.084	1142	73	∞	37	7	0.743	7.00
1999	46	15.1	0.824	0.676	0.188	∞	220	∞	44	5	0.427	4.82
2000	194	14.1	0.803	0.698	0.129	∞	9,130	∞	124	6	0.392	4.35
2001	128	14.8	0.796	0.72	0.097	1313	331	∞	122	10	0.609	7.19
2002	389	14.5	0.782	0.681	0.125	1739	755	∞	387	9	0.630	5.23
2003	169	14.7	0.806	0.71	0.122	1282	366	∞	167	9	0.524	5.89
2004	162	14.7	0.809	0.738	0.092	515	279	2,119	161	11	0.620	7.47
2005	394	14.7	0.805	0.725	0.104	2015	816	∞	396	10	0.610	6.65
2006	383	15.1	0.814	0.726	0.118	2313	946	∞	378	10	0.624	6.67
2007	218	15.1	0.835	0.723	0.144	4237	798	∞	218	10	0.579	6.36
2008	474	15	0.811	0.712	0.125	3578	1,394	∞	466	11	0.571	6.36
2009	476	14.9	0.82	0.689	0.161	3490	1,244	∞	472	12	0.592	6.61
2010	440	15	0.824	0.693	0.162	7758	1,697	∞	433	9	0.641	7.01
2011	362	15.1	0.82	0.725	0.121	∞	3,117	∞	359	11	0.634	6.74
2012	517	15.2	0.817	0.727	0.113	7954	1,892	∞	522	10	0.659	6.71
2013	-	-	-	-	-	-	-	-	-	-	-	-
2014	12	-	-	-	-	-	-	-	-	-	-	-
2015	144	15.1	0.805	0.732	0.092	489	321	951	143	8	0.635	6.47
2016	420	15.1	0.812	0.727	0.106	1798	1,081	4,741	420	9	0.746	7.08
2017	469	14.6	0.811	0.72	0.118	2524	1,388	10,841	469	10	0.647	6.48
2018	443	14.8	0.815	0.72	0.119	3375	1,638	∞	419	10	0.740	7.38
2019	134	14.3	0.808	0.736	0.092	1329	527	∞	134	8	0.677	6.63
2020	426	14.7	0.813	0.729	0.106	1927	1,131	5,627	426	10	0.707	7.28
2021	239	14.7	0.817	0.694	0.148	1263	723	4,219	239	8	0.718	6.65
2022	339	14.7	0.817	0.701	0.143	2301	879	∞	335	9	0.749	6.55
Benchmark		14.8	0.802	0.676	--	--	--	--	--	--	--	--

Table 3. continued

Wild-caught hatchery	N	N_{AC}	H_{EC}	H_{OC}	F_{IS}	N_{eD}	lci	uci	N	N_h	h	H_R
2014	184	14.8	0.831	0.774	0.069	133*	101	184	182	6	0.61	3.87
2015	300	15.43	0.825	0.731	0.115	289	206	443	297	8	0.63	5.25
2016	111	14.23	0.813	0.706	0.144	128	99	173	107	7	0.69	4.61
2019	127	14.00	0.807	0.693	0.145	327	172	1508	127	9	0.68	5.59
Captive spawned												
Global 2016 hatchery	492	14.73	0.821	0.726	0.125	290	184	520	494	9	0.748	5.23
ABP13-003-04 WC	50	13.8	0.808	0.702	0.134	407	190	∞	50	5	0.751	5.00
ABP16-003 CS	39	12.9	0.83	0.743	0.114	79	50	161	39	5	0.533	5.00
Uvalde 2016	100	12.1	0.789	0.700	0.113	47	36	62	100	7	0.745	5.17
16CSDX-003	100	13.2	0.801	0.724	0.102	104	80	141	100	6	0.766	6.10
16CSDX-004	98	10.6	0.801	0.743	0.076	30	25	37	98	6	0.710	5.28
16CSDX-005	100	12.1	0.796	0.732	0.086	55	41	75.4	100	6	0.716	5.09
Global 2017 hatchery	484	13.8	0.812	0.725	0.111	179	120	284	484	10	0.736	5.08
ABP	50	12.4	0.798	0.662	0.182	31	23.7	41	47	3	0.539	3.00
17CSDX-001	98	12.7	0.819	0.721	0.12	171	119	284	98	5	0.710	4.66
17CSDX-002	99	12.8	0.822	0.729	0.116	184	121	753	98	5	0.664	4.82
17CSDX-003	103	13	0.801	0.757	0.055	491	232	∞	102	6	0.707	5.41
17CSDX-004	99	13.2	0.812	0.733	0.097	211	134	432	96	6	0.742	5.54
Global 2018 hatchery	449	13.3	0.815	0.728	0.109	297	214	441	441	6	0.700	6.00

Table 3. continued

Captive spawned	N	N_{AC}	H_{EC}	H_{OC}	F_{IS}	N_{eD}	lci	uci	N	N_h	*h*	H_R
18CSDX-001	197	14.2	0.790	0.701	0.107	334	201	787	196	7	0.711	4.60
ABP16_001_004	50	14.4	0.791	0.682	0.145	103	59	288	50	6	0.56	4.70
ABP18_1CS	49	13.4	0.782	0.701	0.101	573	120	∞	47	7	0.49	5.74
Global 2019 Hatchery	296	14.4	0.804	0.714	0.115	422	286	732	291	8	0.67	5.90
ABP19_CS	50	13.92	0.813	0.701	0.140	78	59	111	50	6	0.635	6.00
DX_YC19	147	13.4	0.796	0.615	0.220	1056	417	∞	147	6	0.727	5.52
Los Lunas released	101	13.87	0.816	0.737	0.100	62	55	72	101	6	0.704	5.78
Global 2020 Hatchery	298	14.58	0.812	0.676	0.170	220	175	286	298	7	0.716	5.02
2021 caplot SNARRC	101	14.31	0.826	0.729	0.126	187	108	510	101	8	0.658	6.35
2021 4WIF1 LLSMR	100	14.15	0.806	0.72	0.109	108	72	188	99	7	0.702	6.88
2021 caplot ABP	48	12.90	0.817	0.742	0.094	81	38	722	48	5	0.652	5.00
2021 Global Hatchery	249	14.57	0.821	0.728	0.118	269	286	443	248	9	0.685	7.68
2022 caplot SNARRC	100	13.93	0.793	0.674	0.146	189	114	442	100	6	0.738	5.38
2022 caplot LLSMR	99	13.17	0.796	0.704	0.120	73	49	123	99	7	0.667	6.19
2022 caplot ABP	50	13.84	0.818	0.680	0.168	59	37	111	50	5	0.642	5.00
2022 Global Hatchery	249	14.17	0.805	0.687	0.146	194	142	284	249	8	0.712	7.41

Table 3. continued

Broodstock	N	N_{AC}	H_{EC}	H_{OC}	F_{IS}	N_{eD}	lci	uci	N	N_h	*h*	H_R
2018 ABQ BioPark-Bs-YC17**	110	14.2	0.808	0.694	0.147	967	314	∞	110	5	0.659	4.73
2018 SNARRC- Bs-YC17**	59	12.7	0.819	0.692	0.158	617	169	∞	59	7	0.728	6.53
2018 ABQ BioPark-Bs-YC18**	123	14.9	0.82	0.729	0.117	385	209	1,095	104	7	0.72	7.2
2018 SNARRC- Bs-YC18**	356	14.2	0.812	0.727	0.109	1,551	370	∞	338	10	0.7	7.07
2019 ABQ BioPark- Bs 2019-YC16/17	191	14.6	0.810	0.689	0.148	2892	569	∞	191	8	0.672	5.96
2019 SNARRC- Bs 2019-YC17	176	12.9	0.790	0.700	0.110	191	222	372	175	8	0.705	5.04
2019 LLSMR- Bs 2019-YC18	186	14.5	0.810	0.719	0.118	449	222	3,338	188	9	0.706	5.49
2020 ABQ BioPark-Bs-YC15	100	14	0.808	0.7	0.14	406	242	1,083	101	5	0.499	4.71
2020 ABQ BioPark-Bs-YC18	99	14.4	0.799	0.719	0.10	615	306	10,399	100	7	0.687	6.29
2020 SNARRC- Bs_YC17	99	15	0.827	0.744	0.100	160	124	217	99	8	0.665	6.68
2020 SNARRC- Bs_YC18	100	14.8	0.805	0.678	0.15	477	265	1,832	100	8	0.709	7.37
2020 SNARRC- Bs_YC19	96	15.5	0.821	0.738	0.100	495	239	2,047	97	9	0.649	7.13
2020 LLSMR-Bs-ABP18-4WI	138	15.6	0.833	0.731	0.112	∞	2,285	∞	137	10	0.740	7.48
2021 ABQ BioPark-Bs-YC16	98	14.83	0.813	0.703	0.128	1,289	276	∞	98	8	0.670	7.25
2021 ABQ BioPark-Bs-YC19	199	15.05	0.818	0.714	0.129	2,225	686	∞	199	10	0.722	7.66
2021 ABQ BioPark-Bs-YC20	258	14.87	0.813	0.715	0.124	3,255	722	∞	258	10	0.710	6.45
2021 SNARRC- Bs-YC20	199	15.02	0.810	0.705	0.131	∞	296	∞	198	10	0.725	6.83
2021 LLSMR-Bs-YC19	50	15.29	0.827	0.747	0.099	1,072	383	∞	50	8	0.799	7.96
2021 LLSMR-Bs-YC20	149	14.64	0.806	0.723	0.104	3,046	625	∞	148	9	0.706	7.28
[1]2022 ABQ BioPark-Bs-1	95	14.24	0.818	0.709	0.134	∞	388	∞	95	8	0.727	7.44
[2]2022 ABQ BioPark-Bs-2	95	15.42	0.817	0.704	0.144	∞	397	∞	95	9	0.724	7.86
[2]2022 ABQ BioPark-Bs-3	95	14.93	0.811	0.706	0.133	1,726	294	∞	95	7	0.729	6.25
[3]2022 ABQ BioPark-Bs-4	95	14.77	0.812	0.700	0.141	832	249	∞	95	8	0.741	6.89
[4]2022 ABQ BioPark-Bs-5	95	14.73	0.804	0.716	0.112	∞	376	∞	95	9	0.707	7.34
[5]2022 ABQ BioPark-Bs-6	93	13.86	0.816	0.702	0.144	656	196	∞	95	7	0.762	6.43
2022 SNARRC-Bs-YC19	95	14.36	0.812	0.680	0.166	500	227	∞	95	9	0.777	7.96
2022 SNARRC-Bs-YC20	94	14.07	0.813	0.696	0.150	853	223	∞	95	8	0.674	7.08
2022 LLSMR-Bs-WC20	95	14.95	0.814	0.729	0.104	4,933	502	∞	95	8	0.760	6.61
2022 LLSMR-Bs-WC21	94	13.97	0.805	0.673	0.159	978	276	∞	94	9	0.754	8.14

[1]ABP19-3Wild-Angostura/ABP19-4-Wild-SanAcacia/ABP20_5Wild_Isleta; [2]ABP20-4-Wild-San Acacia; [3]ABP21-2-Wild-Angostura; [4]ABP21-2 Wild San Acacia; [5]ABP21-3-Wild-Isleta

Figure 1. Annual diversity metrics (1999-2022) calculated from microsatellite loci and mtDNA. Estimates of gene diversity and heterozygosity obtained from resampling of microsatellites (H_{EC} and H_{OC}) and haplotype diversity (*h*) from mitochondrial data are shown in the lower panel, and number of alleles (N_{AC}) is shown in the upper panel. Dashed (H_{EC}) and dotted (H_{OC}) lines indicate diversity benchmarks obtained using a resampling procedure and correspond to a minimum sample size of n=43. These plots show the diversity values obtained by resampling without the small 1987 sample.

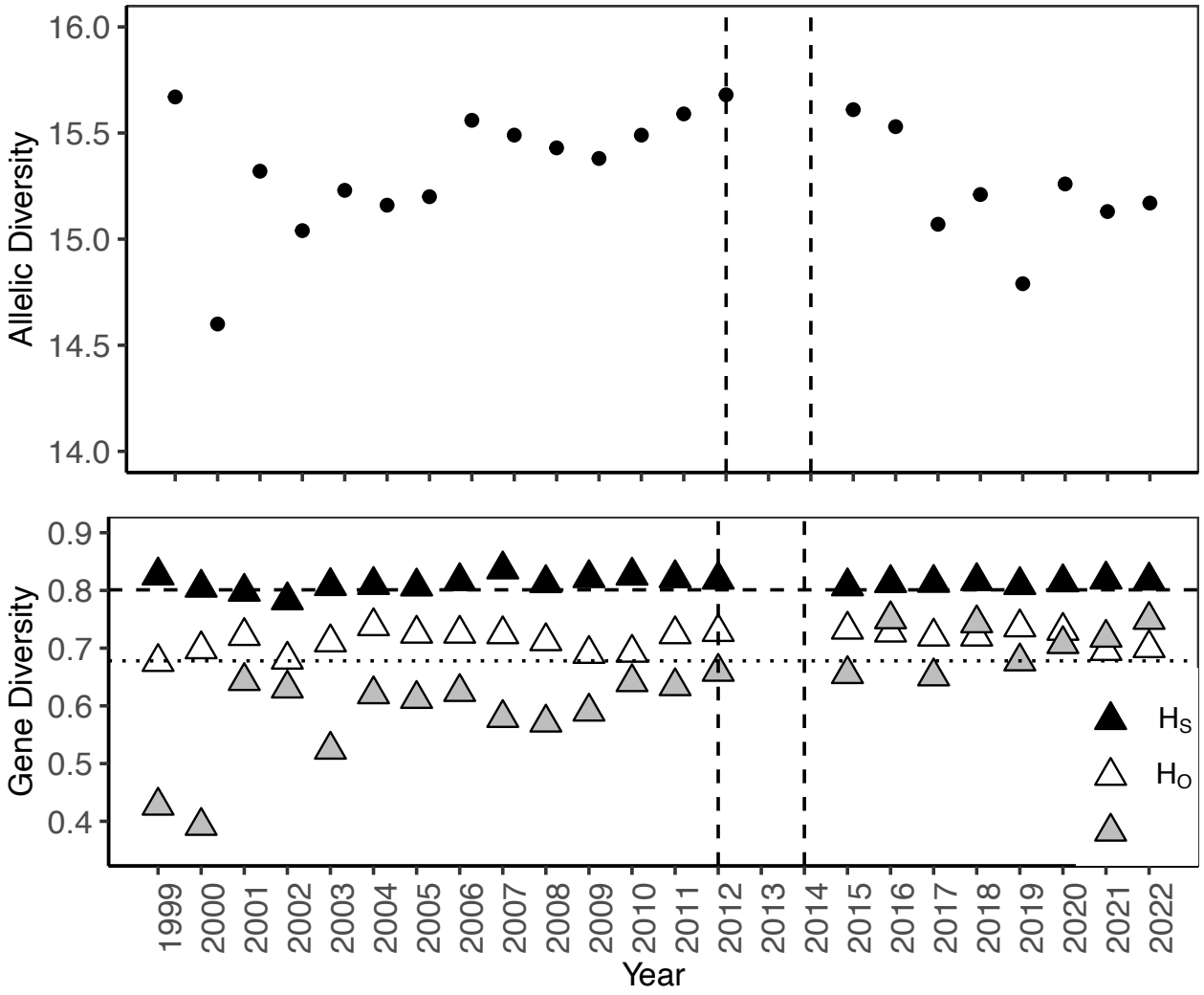

Figure 2. Annual diversity metrics of wild Rio Grande Silvery Minnow by reach (Angostura, Isleta, San Acacia). Microsatellite and mtDNA diversity estimates, gene diversity (H_{EC}), haplotype diversity-*h*, top), heterozygosity (H_{OC}, middle), allelic diversity (bottom) were corrected for differences in sample sizes across years by resampling. Dashed/dotted lines indicate benchmark values for H_{EC}, H_{OC} and N_{AC}.

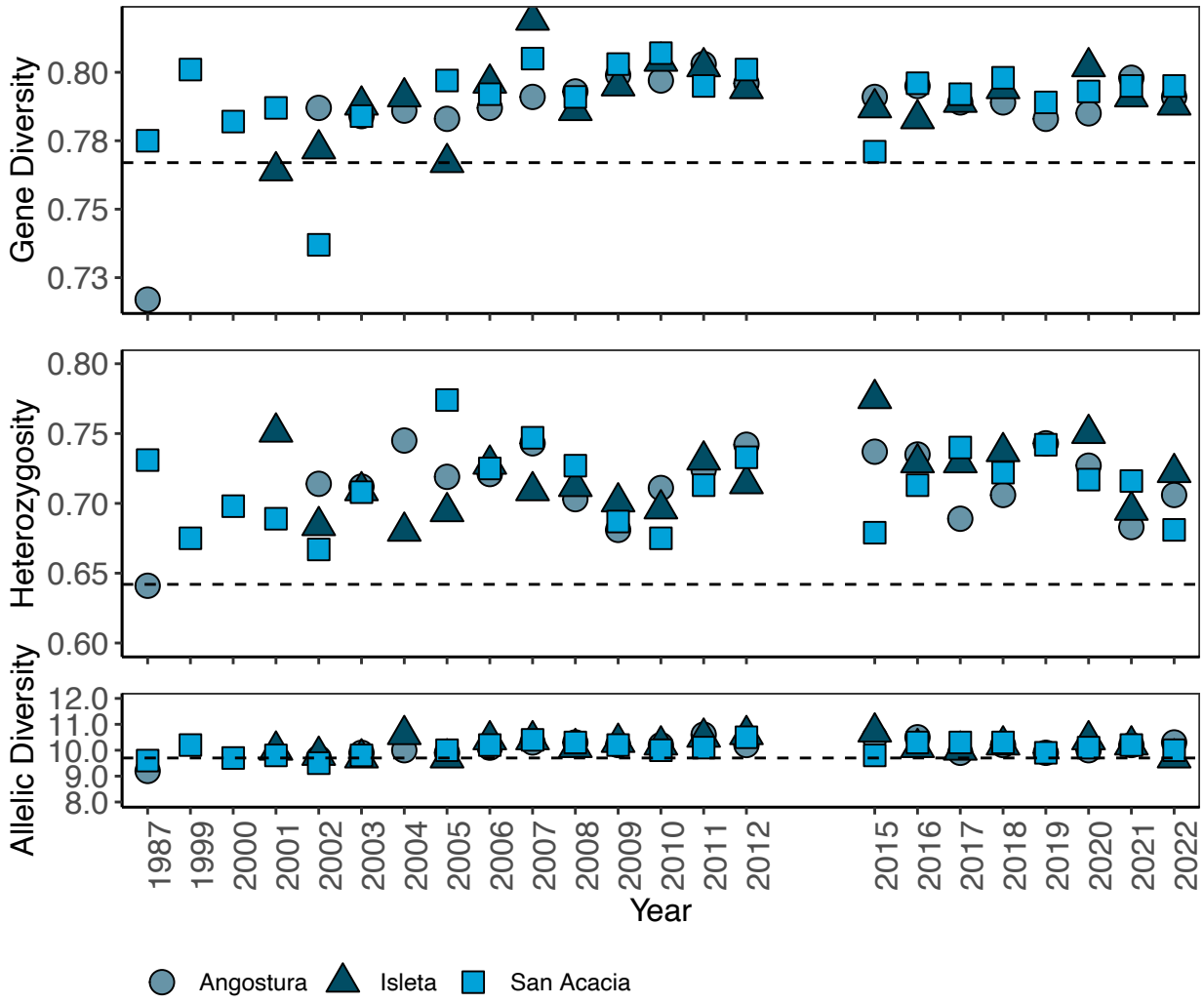

Figure 3. Annual mtDNA diversity metrics of wild Rio Grande Silvery Minnow by year and river reach. Estimates of mtDNA haplotype diversity are shown in the upper panel and haplotype richness are shown in the lower panel.

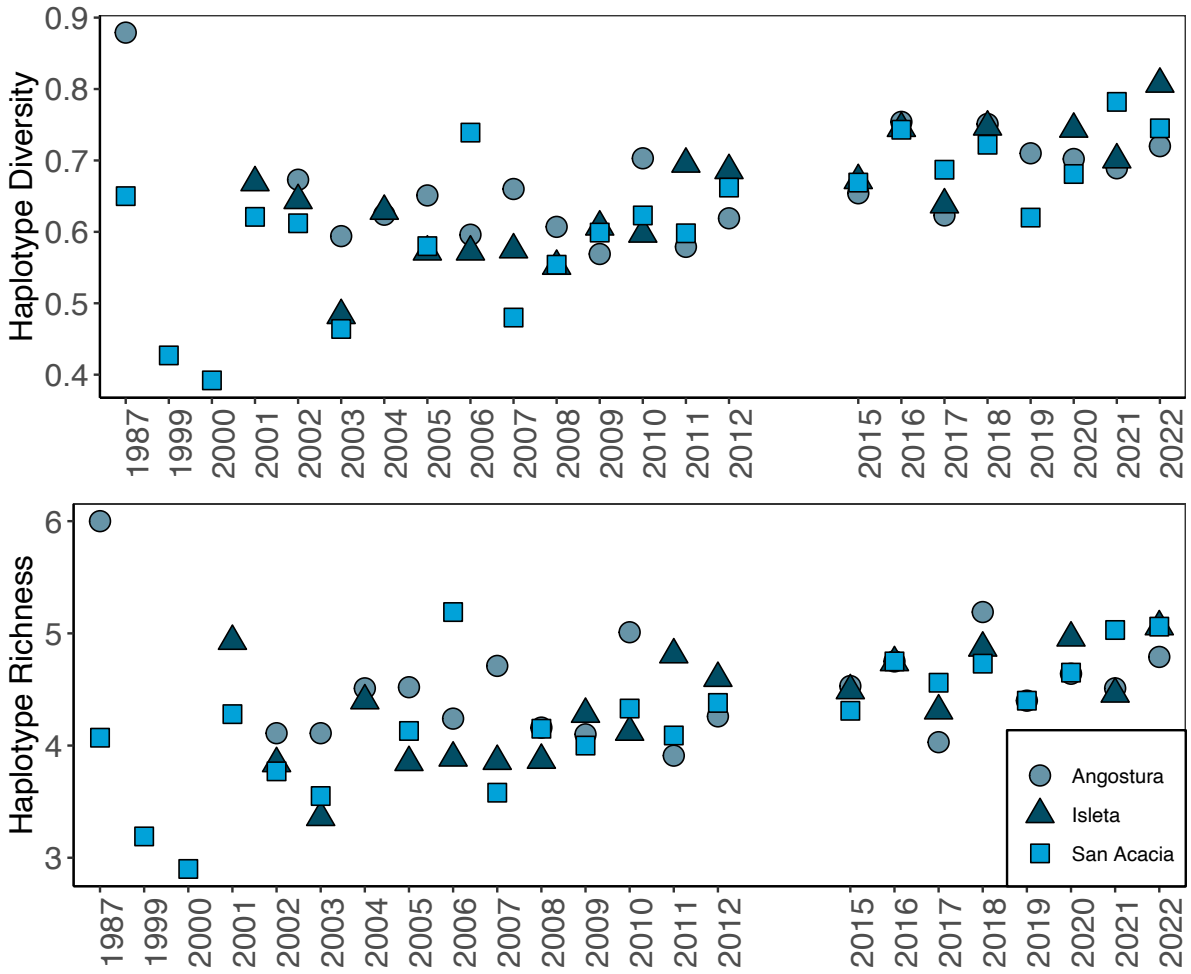

MtDNA- genetic diversity

A total of 17 mtDNA haplotypes have been identified from assaying 6,873 wild (untagged) individuals from the middle Rio Grande from 1987 to 2022 (Table 4). Haplotype A was the most common in almost all samples including the 2022 collections. In the 2022 wild-collected samples, haplotype A was present in 41% of individuals, haplotypes C, D, O were present at moderate frequencies and five haplotypes (E, I, K, F, M) were uncommon. For the first time since genetic monitoring commenced, haplotype E was not detected in the Middle Rio Grande population in 2021 and only a single individual was detected with this haplotype in the 2022 wild-collected sample. Likewise, haplotype E was not detected in the fishes that were released to the river in the fall of 2021 and this haplotype is very rare (<2%) in the refugial broodstocks. At the reach level in 2022, seven to eight haplotypes were detected and mtDNA diversity statistics; identical to the results from 2021 (Figure 3). Across the time series, *h* exceeded 0.7 in the 1987, 2016, 2018, 2020 and 2021 samples and was the lowest in 2000 (h = 0.392) (Table 3, Figure 3). In 2022, *h* ranged from 0.749 ('wild') to 0.674 (22SNARRC-Bs-YC20). Haplotype richness in 2022 'wild' samples decreased compared to 2021 (Figure 3; Table 3) while *h* increased slightly. Haplotype diversity and H_R were marginally higher in the Isleta reach (h= 0.807, H_R= 5.06) compared to the Angostura reach (h=0.72, H_R= 4.79) in 2022. In 2022, two rare haplotypes (I and V) were detected in a small number of hatchery individuals but only haplotype I was detected in the 2022 wild sample. In the Albuquerque BioPark broodstocks, seven to nine haplotypes were present, nine haplotypes were observed in the Southwestern ARRC broodstocks and nine haplotypes were detected in the LLSMR broodstocks (Table 5).

Population structure- microsatellites

In 2022, there were no significant differences between Rio Grande Silvery Minnow collected from the Angostura and Isleta reaches (F_{ST}=0.002 [-0.002 – 0.007]). Small by significant values of pairwise F_{ST} occurred between both Angostura and Isleta reaches when compared to fish from the San Acacia reach (F_{ST}=0.007 [0.004 – 0.012]; F_{ST}=0.013 [0.007 – 0.021) following Bonferroni correction. Total population structure was evaluated by considering global F_{ST} estimates across 2022 samples, including hatchery stocks and broodstock (Figure 4A). For this analysis, we also included samples from 2020 and 2021. Samples from the middle Rio Grande (likely a combination of wild-born and untagged hatchery origin fish) collected in 2022 differed significantly from almost all captive stocks (released and refugial broodstocks). There was also significant variance in allele frequencies among most captive stocks.

The DAPC plot reveals a general contraction on group distribution (i.e., variability within years) until 2012 with higher variability detected in 2000 and 2005. From 2015 onwards, there is a change in group distributions along the first discriminant axis (Figure 5). These results indicate a small and gradual decrease in variability within years prior to the 2013-2014 population bottleneck and shifts of allele frequencies that occurred after the bottleneck.

Population structure- mtDNA

Across the time series, samples collected from the Angostura, Isleta, and San Acacia reaches were not significant (Φ_{CT} = -0.0003, p = 0.422). Likewise, pairwise Φ_{ST} between reaches in 2022 were small and not significantly different from zero (Angostura and Isleta: Φ_{ST}=0.021, p-value = 0.045, Φ_{ST}= 0.004, p-value = 0.261 between Isleta and San Acacia). For the comparison between Angostura and San Acacia Φ_{ST} was also small (Φ_{ST}=0.013) but significantly different from zero (p-value = 0.009). Total population structure was evaluated using Φ_{ST} estimates across all 2022 samples, including hatchery stocks and refugial

broodstock (Figure 4B) based on mtDNA haplotype frequencies. We also included the 2020 and 2021 sample collected from the middle Rio Grande population. After Bonferroni correction, there were nine significant pairwise comparisons including between the 2021 and 2022 middle Rio Grande samples (Φ_{ST}=0.023, p < 0.0001).

Genetic effective population size

Microsatellite-based estimates of N_{eV} are shown in Figure 6-7. Estimates for 2021-2022 based on wild-collected individuals ranged from 230-530; an increase from the previous time period (2020-2021). Estimates of immigration rates from the hatchery to wild population were variable across the time-series ranging from 0.087 (2015-2016) to 0.430 (2020-2021; Figure 8). Average estimates of *m* almost doubled for 2012-2022 period compared the decade preceding the 2012-2014 population bottleneck (2002-2012: $\overline{m}$ =0.166; 2012-2022: $\overline{m}$=0.29). Across the time-series, MLNe estimates that included input of hatchery-reared individuals were smaller than wild-only samples. The 2021-2022 sample MLNe (wild + hatchery) estimate was 243; an increase from the previous temporal sample.

Inbreeding effective size (N_{eD}- effective number of parents) was 2,301 (95% CI 879-∞) for wild fish collected in 2022; almost twice the 2021 estimate (Figure 9; Table 3). N_{eD} for captive stocks released in the middle Rio Grande in 2021 from the Albuquerque BioPark and LLSMR values were small (N_{eD}=59-73) while for fish released from Southwestern ARRC N_{eD} was 189. Across facilities, estimates of N_{eD} from refugial broodstock were large (>500). These values reflect the effective size of the generation preceding the broodstock samples.

MLNe estimates of female variance effective size, N_{ef}, based on mtDNA are shown in Figure 10. For 2021-2022 temporal comparison, estimates of N_{ef} increased from the previous time period to N_{ef} = 147 (95% CI 49-∞).

DISCUSSION

Genetic monitoring

Monitoring genetic diversity parameters (H_E, H_O, A_R and N_e) across contemporary time-series can illuminate demographic and evolutionary processes affecting wild and captive populations that are unattainable using standard demographic sampling approaches. To our knowledge, data from Rio Grande Silvery Minnow is one of the longest genetic monitoring time-series for any non-salmonid freshwater fish; spanning more than three decades and comprising 24 temporal samples (1987, 1999-2012, 2015-2022). Annual monitoring of the genetic status of both 'wild' Rio Grande Silvery Minnow in the middle Rio Grande in addition to representative captive stocks repatriated to the river allows assessment of whether management actions are maintaining levels of genetic diversity in the species. Maintenance of diversity is critical because genetic diversity facilitates adaptation and responses to changing conditions.

Status of the 'wild' (i.e. untagged) Rio Grande Silvery Minnow population in 2022

The population monitoring program for Rio Grande Silvery Minnow (1993-2022) shows that the wild population has experienced multiple, order-of-magnitude changes in density over the past two decades (Dudley et al. 2021). The period from 2015-2017 saw abundances of Rio Grande Silvery Minnow increase substantially over values recorded between 2012-2014; demonstrating the capacity of the species to rebound

rapidly following periods of very low density. Subsequently, there was a >99% decline in estimated density between 2017 and 2018 (Dudley et al. 2018) associated with extensive channel drying (> 60 km) between April through October 2018 and almost complete recruitment failure (Archdeacon et al. 2020a). This occurred as a result of a period of moderate to severe drought that extended from December 2017 to February 2019 (Archdeacon et al. 2020a). In 2019, the population increased 2,285% over densities seen in the previous year. This population response was associated with extended high spring flows and minimal channel drying and strong recruitment (Dudley et al. 2020; Archdeacon et al. 2020a). However, October sampling in 2020 revealed another substantial population decline (-88.8%) (Dudley et al. 2021) with only a marginal increase by October 2021 (Dudley et al. 2022). Repeated changes in population size, particularly repeated bottlenecks, are expected to gradually erode genetic diversity in the absence of actions to buffer the population (i.e., supportive breeding and augmentation) and eventually diversity will likely be lost despite these actions. From 1987 and 1999-2004, both microsatellites and mtDNA showed considerable inter-annual variability in gene diversity metrics and effective population size estimates. Following commencement of population supplementation with fish reared in captivity, inter-annual variability in diversity measures decreased from 2005 to 2012 and during this period there were marginal increases in mtDNA and microsatellite diversity. From 2006 to 2012 and 2015-2016 allelic diversity remained above the benchmark for this metric. More recently (2017-2022) this diversity measure has been at or below the benchmark (Table 3). These results demonstrate that the augmentation program has been critical in maintaining diversity in the face of repeated population bottlenecks. However, results also emphasize the importance of maintaining large and diverse captive stocks and maximizing the number of individuals used for captive breeding.

Genetic effective population size

Genetic effective population size is a key parameter in genetic monitoring programs because N_e determines the amount of variation that is transmitted to the next generation and at smaller N_e, diversity is lost more rapidly. Genetic effective population size estimates based on changes in allele frequencies from one year to the next revealed a substantial decline in 2021 with N_{eV} and N_{ef} estimates among the lowest (<100) since genetic monitoring began reflecting strong genetic drift in allele frequencies between the breeding populations in 2020 and 2021. In 2022, N_{eD}, N_{eV} and N_{ef} both increased compared to 2020-2021, implying more favorable conditions for Rio Grande Silvery Minnow. We also estimated N_{eV} of the entire population (wild and augmented and referred to as N_{eT}) fish to understand the consequence of ignoring the contribution of augmented fish. Across the time-series, estimates of N_{eT} were generally less than half of the wild-only estimates; implying that augmentation of the MRG population with captive-reared fish imposes an additional source of genetic drift. Reproductive contributions of wild and hatchery components of the Rio Grande Silvery Minnow population may vary considerably from year to year depending upon environmental conditions that drive fluctuations in abundance and in turn dictate management actions (Dudley et al. 2020; Yackulic et al. 2022). Even moderate levels of gene flow between wild and hatchery populations can reduce N_e particularly when the wild-born population is small and the hatchery fish (derived from relatively few breeders) comprise a larger component of the population. This occurs via breeding between individuals derived from relatively few adults, changing allele frequencies rapidly and reflected by small N_e. Smaller N_e estimates (MLN_e and N_{eD}) when the fraction of hatchery to wild-born fish is higher are consistent with expectations of a Ryman-Laikre effect (Ryman & Laikre 1991). Theoretical studies showed that in large wild populations, captive propagation can drastically reduce N_e unless captive contribution is very small or if wild N_e is a tiny fraction of census size (< 0.0001) and the impacts to N_e would be exacerbated in situation of repetitive supportive breeding (Waples et al. 2016), as in Rio Grande Silvery Minnow. However, potential

interactions between wild and hatchery components of the population are complex and understanding the implications for estimating N_e is not straightforward (e.g., Gilbert and Whitlock 2015).

Figure 4 A. Values of F_{ST} based on microsatellites and **B**. Values of Φ_{ST} based on mitochondrial DNA haplotype frequencies between wild collected, released captive-reared and refugial Rio Grande Silvery Minnow populations. Significant values are indicated by black asterisks.

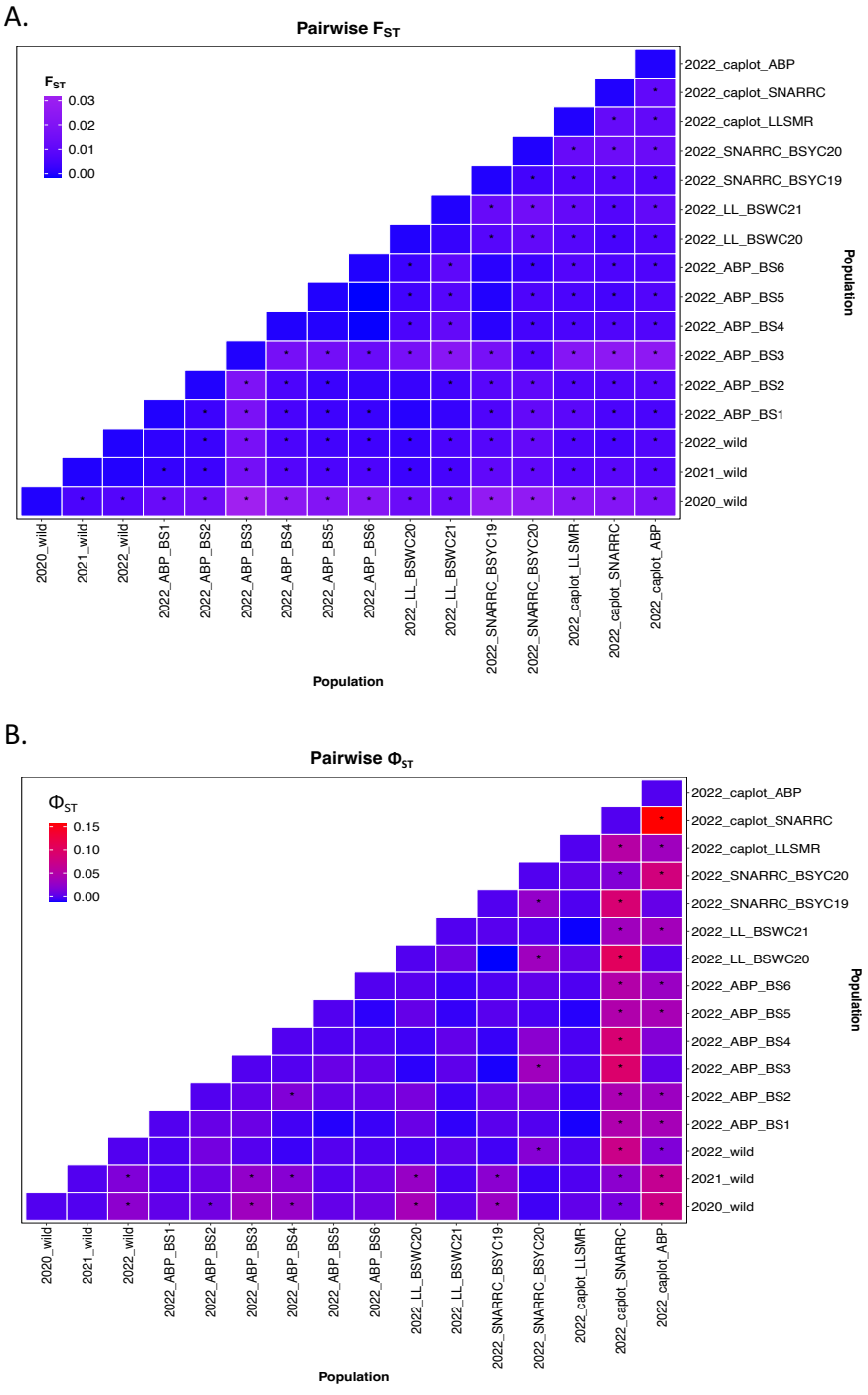

Figure 5. Results of discriminant analysis of principal components (DAPC) showing the ellipses representing the 95% confidence level for a multivariate normal distribution, plotted along the first and second discriminant functions (DFs) axes. The first DF explained 22.3% of the variance and the second explained 11.3%. Colors represent temporal samples.

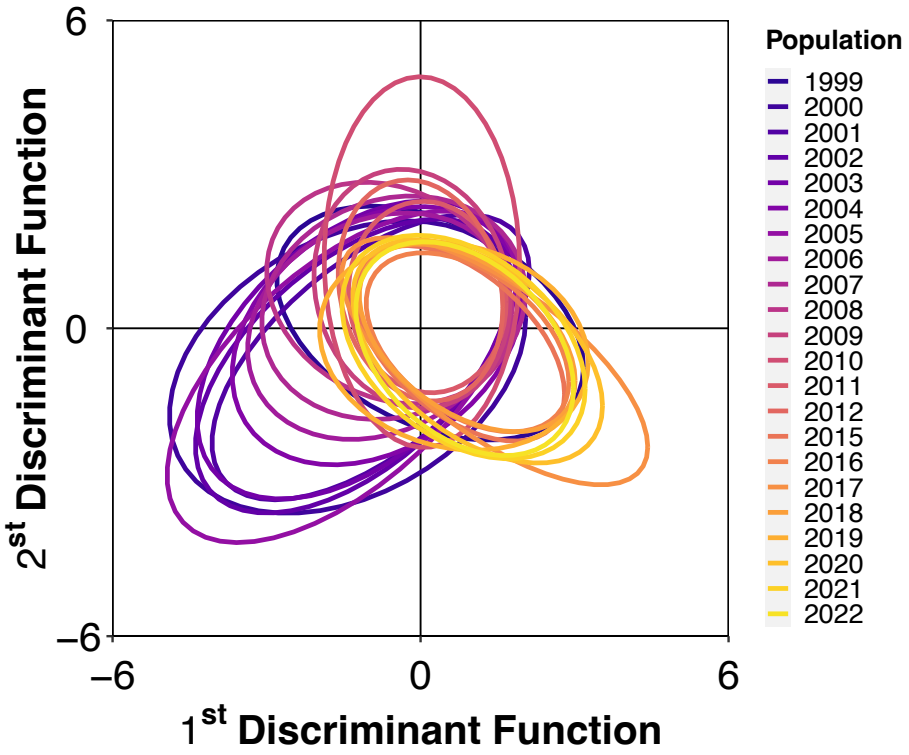

Figure 6. Variance effective size (N_{eV}) calculated from microsatellite data from wild samples estimated with the method of (**A**) Nei-Tajima and (**B**) Jorde-Ryman. Associated 95% CIs are shown. Upper error bars extending to y-maxima indicate infinite upper estimate bounded 95% CI.

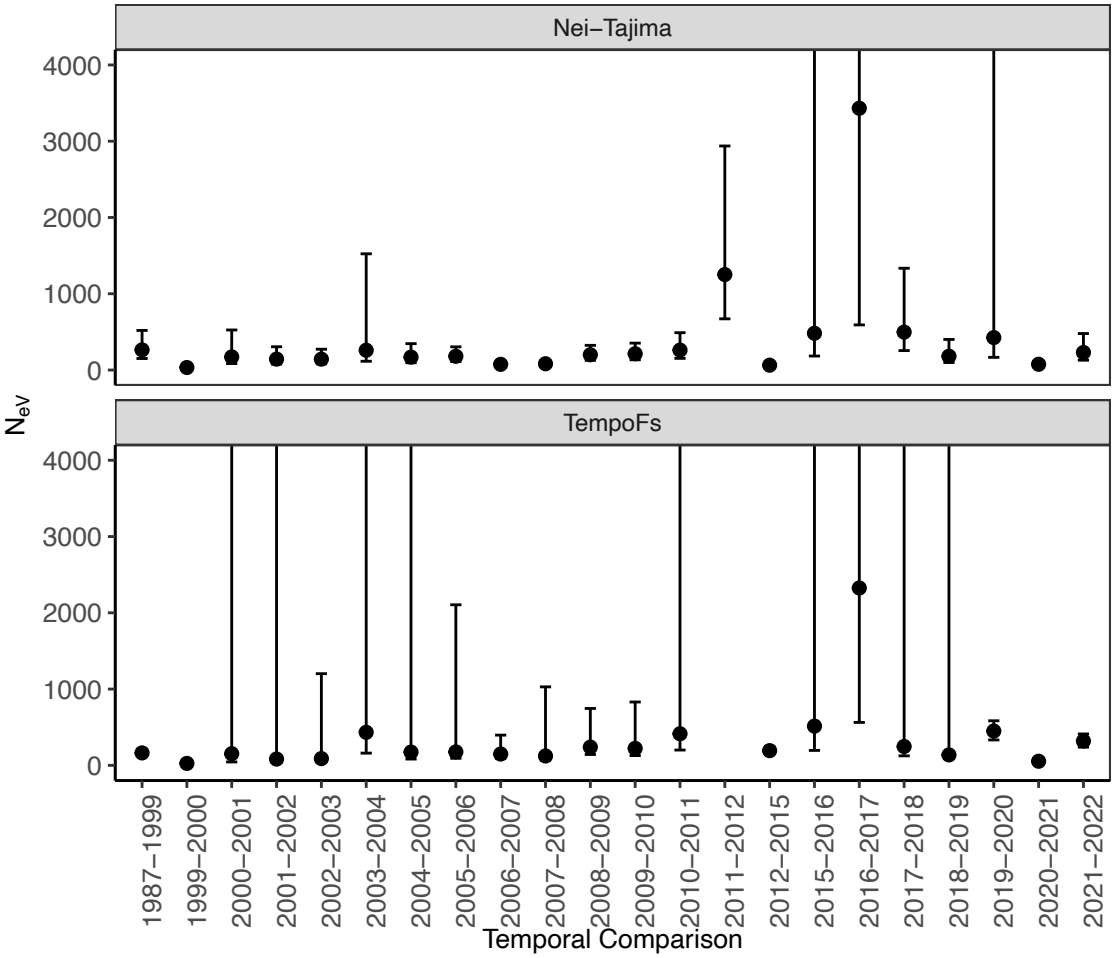

Figure 7. Variance effective size (N_{eV}) calculated from microsatellite data, as based on MLNe estimates (**A**) of wild-only samples and incorporating the input of fish released from the hatcheries (red points) (**B**) and their associated 95% CIs. Upper error bars extending to y-maxima indicate infinite upper estimate bounded 95% CI. The dashed lines indicate N_e=50 and N_e=500. These values have been proposed as targets to avoid negative impacts of inbreeding (N_e=50) and loss of genetic variation via genetic drift (N_e=500).

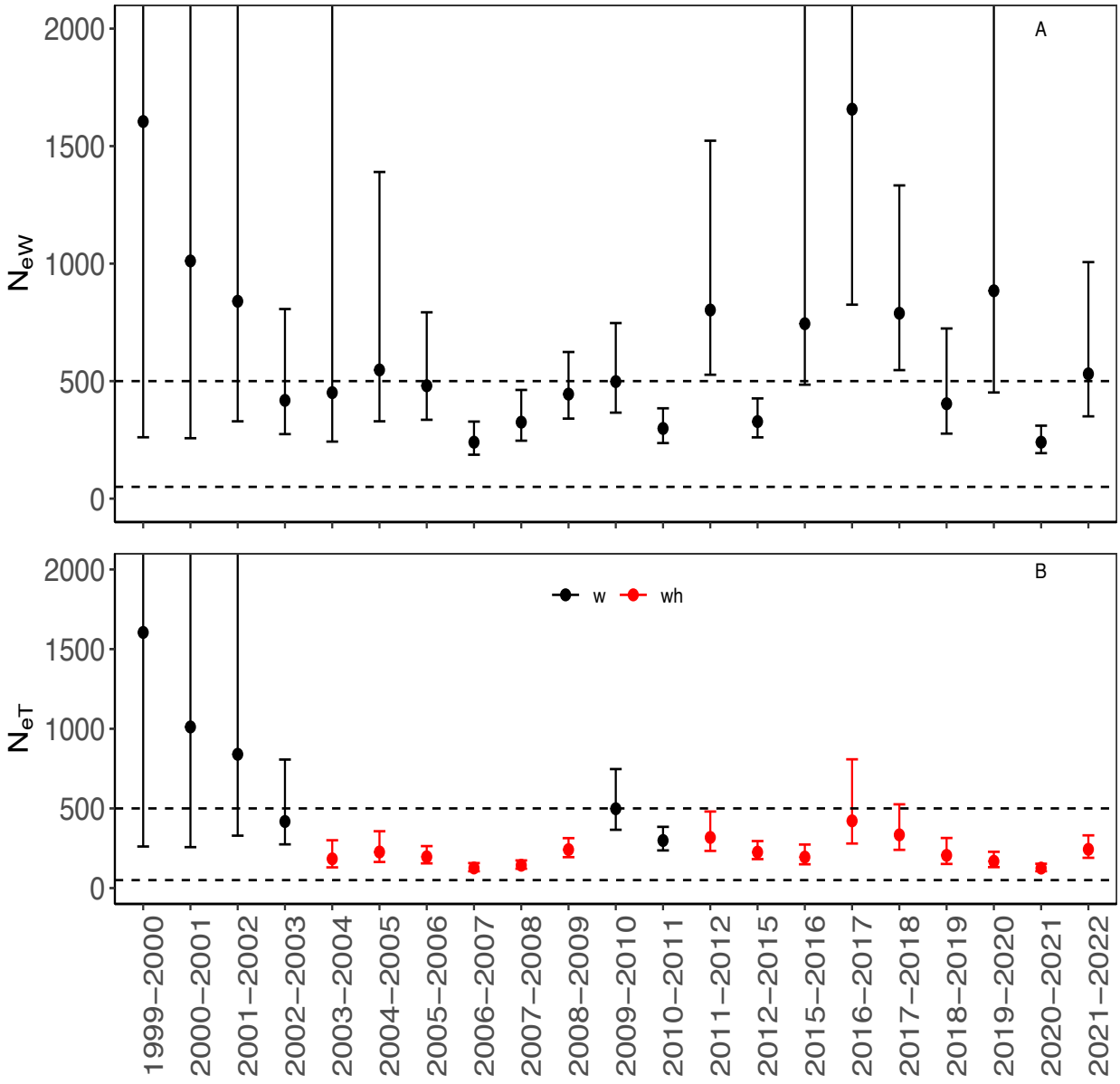

Figure 8. Genetic estimates of immigration (*m*) of hatchery-reared individuals to the middle Rio Grande population. The entire time-series is included but note that augmentation did not commence until 2003 and there was limited augmentation in 2009-2010.

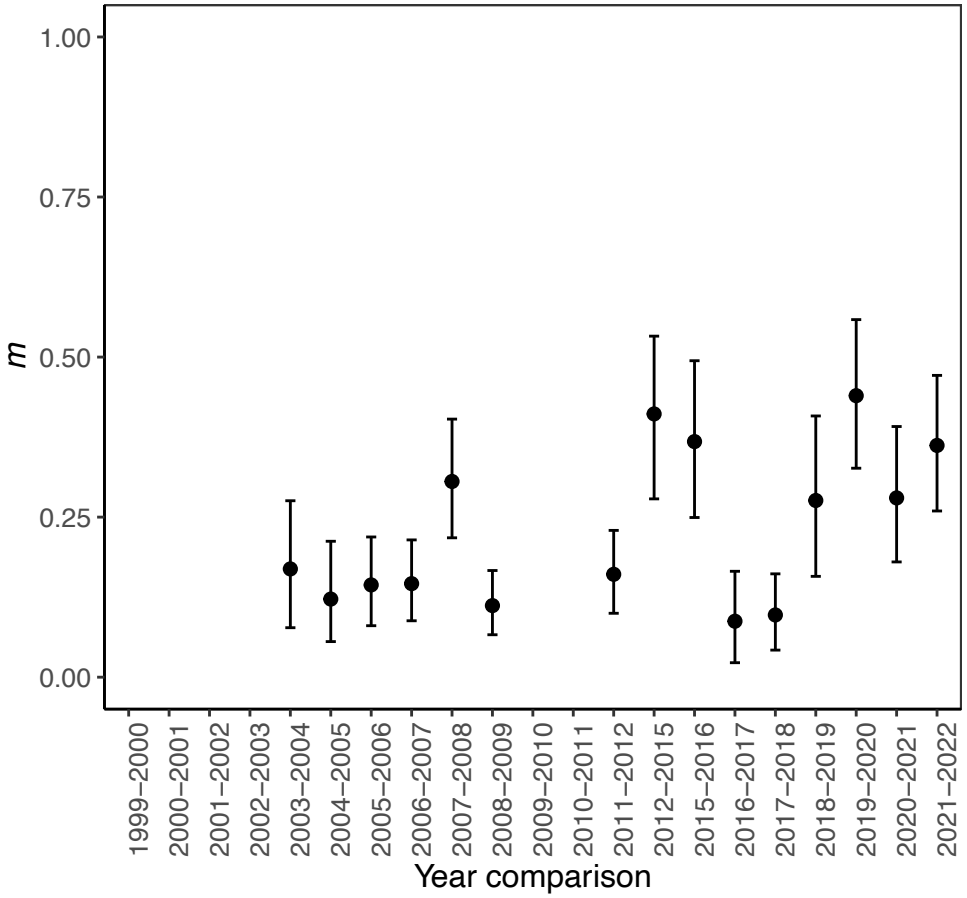

Figure 9. Estimates of inbreeding effective size (N_{eD}) and their associated 95% confidence intervals. Note the logarithmic scale on y-axis. Infinite mean estimates are indicated by points lying at y-maximum, and upper error bars extending to y-maximum indicate infinite upper bounded 95% CI.

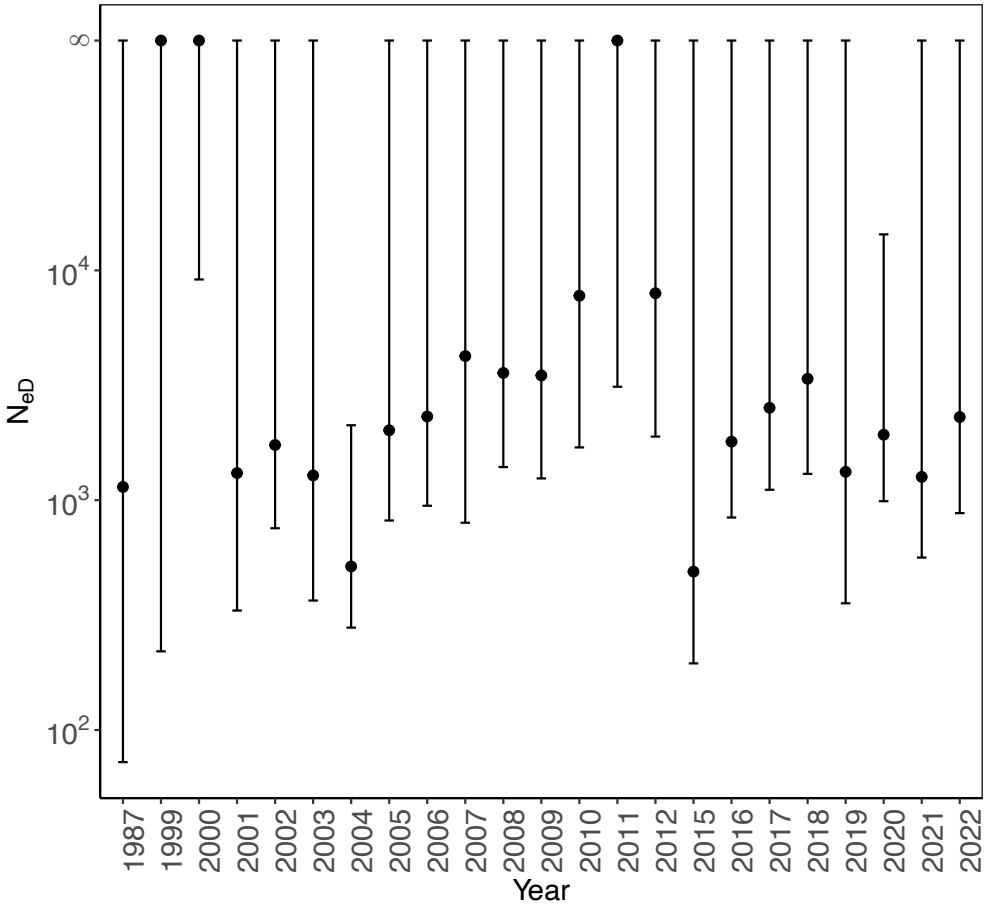

Figure 10. Female variance effective size estimates (N_{ef}) and associated 95% CIs, based on mtDNA data and calculated using MLNe (upper) method. Infinite mean estimates are indicated by points falling outside of the plot area and upper error bars extending to y-maxima indicate infinite upper bounded 95% CI.

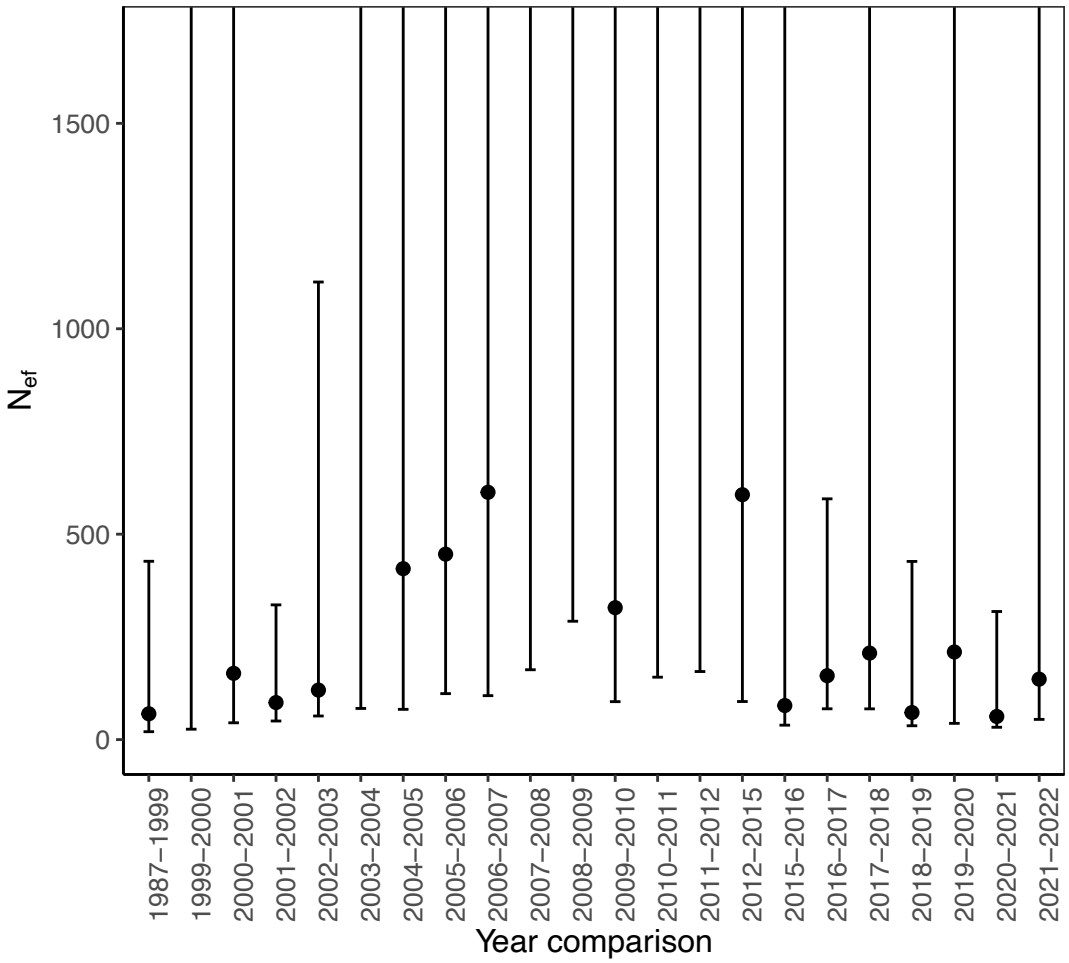

Importantly, there has also been a steady decline in N_{eT} since 2016-2017. In 2019, it was estimated that more than two-thirds of the population were of hatchery origin; increasing the likelihood of breeding between related individuals the following year. Smallest values of N_{eT} occurred in more recent temporal comparisons (2019-2020 and 2020-2021); consistent with demographic data showing a substantial population decline in October 2020 and substantial gene flow from the hatchery to the middle Rio Grande population (m = 0.439). Supportive breeding in the face of repetitive collapses of the wild population, act together to decrease N_e. Larger values of N_{eT} and N_{eW} in 2021-2022 is a positive outcome.

Linkage disequilibrium effective size (N_{eD}=2,301) also increased in 2022 from 2021 values (N_{eD}=1,263). It is important to reiterate that N_{eD} estimates reflect the effective size of the parental generation of the sample. Hence, the increase in effective size reported in 2022 reflects an increase in the size of the breeding population in 2021. From a management perspective, there are a number of theoretical and practical distinctions between N_{eI} (inbreeding effective size, to which N_{eD} estimates are most closely associated) and N_{eV} (variance effective size). These two measures of effective size should be similar in stable populations but show predictable differences in declining or growing populations. In declining populations N_{eI} should be larger than N_{eV} because the latter depends on the amount of genetic drift between sampled generations but the former is a measure of inbreeding in the generation prior to sampling, (Allendorf & Luikart 2007); therefore, N_{eI} is only reduced once mating between close relatives becomes more common (i.e., homozygosity increases in the population). Across the time-series we observe a disparity between N_{eD} and N_{eV} and this trend continued in 2022. Carson et al. (2020) investigated the relationship between N_{eD} and N_{eV} using simulations and showed that the disparity between N_{eV} and N_{eD} is driven by the interaction of population augmentation and fragmentation. N_{eV}, is negatively associated with both bidirectional dispersal rates and supplementation relative to equilibrium N_e while N_{eD} reflects the total population size including the augmented (i.e., hatchery-derived) component.

Genetic diversity of captive stocks released to the middle Rio Grande, New Mexico

In November/December 2021, ~204,000 fish were released in the middle Rio Grande, New Mexico. Gene diversity and heterozygosity for pooled captive lots released to the Rio Grande in November/December 2021 were greater than the lower 95% CI genetic diversity benchmark. Some diversity metrics fell below the benchmark estimates in individual captive stocks released in November/October 2021. In 2022, mitochondrial haplotype richness (corrected for differences in sample size) was fairly consistent among captive lots and facilities. Preservation of genetic diversity in captive lots is critical because these fish periodically reestablish the species in the middle Rio Grande (e.g., 2014, 2018, 2020). The apparent failure to detect several mitochondrial haplotypes in the wild population in recent samples, reduced frequency of other formerly moderately common haplotypes (i.e., E), absence of several haplotypes in captive stocks and small effective population size of some captive stocks suggest that genetic drift is eroding diversity in the genome.

Genetic Analysis of Broodstock

In 2022, we genotyped fish representing the 2019, 2020, 2021 broodstock year classes. All measures of genetic diversity in these stocks were very similar to estimates in the middle Rio Grande population. However as in previous years, haplotype representation and frequencies of rare haplotypes differed between lots and facilities, such that not all haplotypes were identified in all refugial populations. This result highlights the continued need to maintain multiple refugial populations across different facilities and the importance of spawning large numbers of individuals to preserve rare alleles.

CONCLUSIONS

More than two decades of genetic monitoring of the 'wild' middle Rio Grande population and of released captive reared/bred Rio Grande Silvery Minnow provides a rare opportunity to track the genetic effects of population fluctuations associated with inter-annual variability in flows and of key management activities. The results presented here indicate that the trajectory of genetic change in the wild Rio Grande Silvery Minnow population is now determined largely by supplementation with captive reared stocks. Higher estimated rates of gene-flow from the captive-reared component of the population into the middle Rio Grande population highlights the importance of maintaining genetically diverse captive stock and using large numbers of adults in captive spawning. Critically, it is also important to maximize collection of wild produced eggs in years when flow conditions are suitable such that genetic contributions of many adults are represented in captive stocks. Supplementation buffers the population against potential losses of diversity predicted by drastic changes in population size (Osborne et al. 2012). The most sensitive metric of genetic diversity (allelic diversity) demonstrates that N_{AC} was maintained through 2016, but since, values of N_{AC} declined, and in 2021-2022 observed heterozygosity was also reduced. Likewise, recent analysis with SNP-based microhaplotypes indicates increases in values for alternative metrics of inbreeding (Osborne et al. In Press). These results highlight the importance of continued monitoring of both released captive stocks, broodstocks and the middle Rio Grande population as any detrimental effects (such as losses of diversity) in the captive stocks will ultimately be transferred to the 'wild' population particularly when there are high rates of gene flow between wild and captive population components. Transitioning genetic monitoring to the SNP-based GT-seq panel will also provide an important tool for understanding the interaction between wild-born and captive-reared population components on levels of inbreeding in the population.

ACKNOWLEDGEMENTS

We gratefully acknowledge the assistance of David Camak, Alexander Cameron, Gregor Hamilton, Huachan Liang, Chloe McGuan (UNM Biology) and Melissa Sanchez (UNM Molecular Biology Core Facility), Emily DeArmon, and curatorial assistants (UNM Museum of Southwestern Biology, Division of Fishes), Manuel Ulibarri and Wade Wilson (USFWS) and Thomas Archdeacon (USFWS), Kathy Lang and Kim Ward (Albuquerque Biological Park), Alison Hutson (Los Lunas Silvery Minnow Refugium) and Jennifer Bachus, Eric Gonzales and Joel Lusk (Bureau of Reclamation).

LITERATURE CITED

Allendorf, F.W., and G. Luikart. 2007. Conservation and the genetics of populations. Blackwell Publishing, Malden, MA, USA.

Archdeacon, T.P. and J.K. Reale. 2020a. No quarter: Lack of refuge during flow intermittency results in catastrophic mortality of an imperiled minnow. *Freshwater Biology*, Early view, https://doi.org/10.1111/fwb.13607

Archdeacon, T. P., Diver-Franssen, T. A., Bertrand, N. G., and Grant, J. D. 2020b. Drought results in recruitment failure of Rio Grande silvery minnow (*Hybognathus amarus*), an imperiled, pelagic broadcast-spawning minnow. *Environmental Biology of Fishes*, 103, 1033–1044.

Bessert, M. L., and G. Ortí. 2003. Microsatellite loci for paternity analysis in the fathead minnow, *Pimephales promelas* (Teleostei: Cyprinidae). *Molecular Ecology Notes,* 3, 532-534.

Bestgen, K. R., and S. P. Platania. 1991. Status and conservation of the Rio Grande Silvery Minnow, *Hybognathus amarus*. *Southwestern Naturalist*, 36, 225-232.

Breiman, L. 2001. Random forests. *Machine Learning*, *45*(1), 5-32.

Carson, E.W., Osborne, M.J. and T.F. Turner. 2020. Relationship of effective size to hatchery supplementation and habitat connectivity in a simulated population of Rio Grande Silvery Minnow. *North American Journal of Fisheries Management*, 40(4), 922-938.

Cook, J. A., K. R. Bestgen, D. L. Propst, and T. L. Yates. 1992. Allozymic divergence and systematics of the Rio Grande Silvery Minnow, *Hybognathus amarus* (Teleostei: Cyprinidae). *Copeia*, 1998, 6-44.

Dimsoski, P., G. Toth, and M. Bagley. 2000. Microsatellite characterization in central stoneroller *Campostoma anomalum* (Pisces: Cyprinidae). *Molecular Ecology*, 9, 2187-2189.

Do, C., R. S. Waples, D. Peel, G. M. Macbeth, B. J. Tillett, and J. R. Ovenden. 2014. NeEstimator V2: re-implementation of software for the estimation of contemporary effective population size (N_e) from genetic data. *Molecular Ecology Resources*, 14, 209-214.

Dowling, T. E., Minckley, W. L., Marsh, P. C., and E. S. Goldstein. 1996. Mitochondrial DNA variability in the endangered razorback sucker (*Xyrauchen texanus*): analysis of hatchery stocks and implications for captive propagation. *Conservation Biology*, 10, 120-127.

Dudley, R. K., S. P. Platania, and G. C. White. 2014. Rio Grande Silvery Minnow Population Monitoring Program results from May to December. Report submitted to the U.S. Bureau of Reclamation Albuquerque Office. 151 pp.

Dudley, R. K., S. P. Platania, and G. C. White. 2018. Rio Grande Silvery Minnow Population Monitoring Program during September 2018. Report submitted to the U.S. Bureau of Reclamation Albuquerque Office. 35 pp.

Dudley, R. K., S. P. Platania, and G. C. White. 2021. Rio Grande Silvery Minnow Population Monitoring Program during 2020. Report submitted to the U.S. Bureau of Reclamation Albuquerque Office. 179 pp. 10.13140/RG.2.2.14448.79360

Excoffier, L., G. Laval and S. Schneider. 2005. Arlequin ver. 3.0: An integrated software package for population genetics data analysis. *Evolutionary Bioinformatics Online*, 1, 47-50.

Frankham, R. 2005. Genetics and extinction. *Biological Conservation*, 126, 131-140.

Goudet, J., and T. Jombart. 2020. *hierfstat:* Estimation and tests of hierarchical F-statistics.

Guo, S. W. and E. A. Thompson. 1992. Performing the exact test of Hardy–Weinberg proportion for multiple alleles. *Biometrics*, 48, 361-372

Hedrick, P. W. 1999. Perspective: Highly variable genetic loci and their interpretation in evolution and conservation. *Evolution*, 53, 313-318.

Hill, W. 1981. Estimation of effective population size from data on linkage disequilibrium. *Genetical Research*, 38, 209-216.

Hillis, D., C. Mable and B. Mable. 1996. Molecular Systematics. Sinauer Associates, Sunderland, MA, USA.

Horwitz, R.J., Keller, D.H., Overbeck, P.F., Platania, S.P., Dudley, R.K. and E.W. Carson. 2018. Age and Growth of the Rio Grande Silvery Minnow, an Endangered, Short-Lived Cyprinid of the North American Southwest. *Transactions of the American Fisheries Society*, *147*(2), 265-277.

Goudet, J., and T. Jombart. 2015. hierfstat: Estimation and tests of hierarchical F-Statistics. R package version 0.04-22. Retrieved from https://CRAN.R-project.org/package=hierfstat

Jombart, T., and Ahmed, I. 2011. adegenet 1.3-1: new tools for the analysis of genome-wide SNP data. *Bioinformatics*, *27*(21), 3070–3071.

Jorde, P. E., and N. Ryman. 1995. Temporal allele frequency change and estimation of effective in populations with overlapping generations. *Genetics*, 139, 1077-1090.

Jorde, P. E., and N. Ryman. 1996. Demographic genetics of brown trout (*Salmo trutta*) and estimation of effective population size from temporal change of allele frequencies. *Genetics*, 143, 1369-1381.

Jorde, P. E., and N. Ryman. 2007. Unbiased estimator for genetic drift and effective population size. *Genetics*, 177, 927-935.

Liaw, A., Wiener, M. (2002). Classification and regression by random forest. *R news*, *2,*18-22.

Laurie-Ahlberg, C. C., and B. S. Weir. 1979. Allozyme variation and linkage disequilibrium in some laboratory populations of *Drosophila melanogaster*. *Genetics*, 92, 1295-1314.

Nei, M., 1987. *Molecular evolutionary genetics*. Columbia university press.

Nei, M., and F. Tajima. 1981. Genetic drift and estimation of effective population size. *Genetics*, 98, 625-640.

Osborne, M. J., S. R. Davenport, C. R. Hoagstrom, and T. F. Turner. 2010. Genetic effective size, N_e, tracks density in a small freshwater cyprinid, Pecos bluntnose shiner (*Notropis simus pecosensis*). *Molecular Ecology*, 19, 2832-2844.

Osborne, M. J., E. W. Carson, and T. F. Turner. 2012. Genetic monitoring and complex population dynamics: insights from a 12-year study of the Rio Grande Silvery Minnow. *Evolutionary Applications*, 5, 553-574.

Osborne, M. J., Caeiro Dias, G., & Turner, T. F. 2022. Transitioning from microsatellites to SNP-based microhaplotypes in genetic monitoring programs: lessons from paired data spanning 20 years. *Molecular Ecology*, Accepted.

Petit, R. J., A. El Mousadik, and O. Pon. 1998. Identifying populations for conservation on the basis of genetic markers. *Conservation Biology*, 12, 844-855.

Pflieger, W. L.1980. *Hybognathus nuchalis* Agassiz, Central silvery minnow. In D. S. Lee, C. R. Gilbert, C. H. Hocutt, R. E. Jenkins, D. E. McAllister, and J. R. Stauffer Jr., eds. *Atlas of North American Freshwater Fishes*, p. 177. North Carolina State Museum of Natural History, Raleigh, NC. Rousset, F., 2008. genepop'007: a complete re-implementation of the genepop software for Windows and Linux. *Molecular ecology resources*, *8*(1), pp.103-106.

Rice, W. R. 1989. Analyzing tables of statistical tests. *Evolution*, 43, 223-225.

Turner, T. F., L. A. Salter and J. R. Gold. 2001. Temporal-method estimates of N_e from highly polymorphic loci. *Conservation Genetics*, 2, 297-308.

Turner, T. F., T. E. Dowling, R. E. Broughton, and J. R. Gold. 2004. Variable microsatellite markers amplify across divergent lineages of cyprinid fishes (subfamily Leusicinae). *Conservation Genetics*, 5, 273-281.

Turner, T. F., M. J. Osborne, G. R. Moyer, M. A. Benavides and D. Alò. 2006. Life history and environmental variation interact to determine effective population to census size ratio. *Proceedings of the Royal Society London B*, 273, 3065-3073.

Schwartz, M. K., G. Luikart, and R. S. Waples. 2007. Genetic monitoring as a promising tool for conservation and management. *Trends in Ecology and Evolution*, 22, 11-16.

U.S. Fish and Wildlife Service., 1994. Endangered and threatened wildlife and plants: final rule to list the Rio Grande silvery minnow as an endangered species. *Federal Register*, 59, 36988–36995.

U. S. Fish and Wildlife Service., 2010. Rio Grande Silvery Minnow (*Hybognathus amarus*) recovery plan, first revision: Albuquerque, New Mexico.

U. S. Fish and Wildlife Service., 2018 Rio Grande Silvery Minnow genetics and propagation management plan, 2018 revision: Albuquerque, New Mexico.

Van Oosterhout, C., W. F. Hutchinson, D. P. M. Wills, and P. Shipley. 2004. MICRO-CHECKER: software for identifying and correcting genotyping errors in microsatellite data. *Molecular Ecology Notes*, 4, 535-538.

Wang, J. L. 2001. A pseudo-likelihood method for estimating effective population size from temporally spaced samples. *Genetical Research*, 78, 243-257.

Wang, J. and M. C. Whitlock, 2003. Estimating effective population size and migration rates from genetic samples over space and time. *Genetics*, 163, 429–446.

Waples, R. S. 1989. A generalized approach for estimating effective population size from temporal changes in allele frequency. *Genetics*, 121, 379-391.

Waples, R. S. 2005. Genetic estimates of contemporary effective population size: to what time periods do the estimates apply? *Molecular Ecology*, 14, 3335-3352.

Waples, R. S., and M. Yokota. 2007. Temporal estimates of effective population size in species with overlapping generations. *Genetics*, 175, 219-233.

Waples, R. S., and C. Do. 2010. Linkage disequilibrium estimates of contemporary N_{eV} using highly variable genetic markers: A largely untapped resource for applied conservation and evolution. Ev*olutionary Applications*, 3, 244-262.

Weir, B. S., and C. C. Cockerham. 1984. Estimating F-statistics for the analysis of population structure. *Evolution*, 38, 1358-1370.

Wright, S. 1931. Evolution in Mendelian populations. *Genetics*, 16, 97-159.

GLOSSARY

Allelic/ haplotype richness – The total number of alleles/haplotypes in a population corrected by rarefaction to account for differences in sample size among collections.

Genetic drift – is the random change in allele frequencies from generation to generation because of sampling error. Specifically, the finite number of genes passed on to progeny will be an imperfect sample of the parental allele frequencies. The effects of genetic drift are (i) allele frequencies will change and (ii) genetic variation will be lost. The smaller the population, the greater the change in allele frequencies due to drift.

Genetic effective size (N_e) – The effective size of a breeding population under idealized conditions meeting the assumptions of Hardy-Weinberg (i.e., equal sex ratio, random mating).

Haplotype/ gene diversity (*h*) – Computationally equivalent to expected heterozygosity (H_e) but referred to as gene/haplotype diversity as there are no heterozygotes because mtDNA is haploid.

Hardy-Weinberg equilibrium – The stable frequency distribution of genotypes (AA, Aa, and aa) in the proportions (p^2, 2pq, and q^2) respectively (where p and q are the frequencies of the alleles, A and a). The Hardy-Weinberg principle makes the following assumptions (i) random mating (i.e. there is neither preference or aversion), (ii) no mutation (i.e. genetic information is transmitted from parent to progeny without change), (iii) large or infinite population size, (iv) no natural selection, (v) no immigration.

Heterozygosity (H_e) – The presence of different alleles at one or more loci on homologous chromosomes. Proportion of heterozygous individuals for a locus in a population.

Inbreeding co-efficient (F) – the probability that two alleles at a locus in an individual are identical by descent. Used to measure the extent of inbreeding.

Linkage disequilibrium – statistical association of alleles at different loci. Such association indicates that two loci are physically adjacent on a chromosome such that there is little recombination during meiosis.

Locus/Loci – A segment of DNA on a chromosome. Loci is the plural form of the noun.

Microsatellite – short tandem repeated DNA sequences e.g. ACACACAC. These loci usually have variable numbers of repeats within/among individuals and high heterozygosity.

Mitochondrial (mt) DNA – maternally inherited circular DNA molecule contained within the mitochondria.

Null allele – a mutation that occurs in a PCR primer site that prevents amplification during polymerase chain reaction (PCR).

Primers – short fragments of DNA that flank the DNA region of interest and which are used in PCR to target specific nuclear and mtDNA loci.

Polymerase chain reaction – method used to make copies through amplification of a specific segment of DNA (such as a microsatellite locus or mitochondrial DNA gene). DNA is heated in the presence of PCR primers, and the Taq polymerase enzyme, to copy the intervening DNA sequencing using ~30 cycles.

Ryman-Laikre effect – an increase in inbreeding and reduction in the total effective population size that can occur in wild-captive systems that occurs when few individuals contribute large numbers of offspring.

Wahlund effect – is a reduction in heterozygosity compared to Hardy-Weinberg expectations, and occurs in a population divided into partially isolated subpopulations

'Wild' vs. 'captive' – we use the term '**wild**' to refer to unmarked fish sampled directly from the Rio Grande. 'Wild' fish may have parents that were wild or bred/reared in captivity, but were hatched in the Rio Grande. The term '**captive**' refers to a fish held in a hatchery or a VIE-tagged fish captured from the Rio Grande. In 2022, we also refer to '**wild-collected**'. These are fish with no tag that were collected in the Rio

Grande in 2021-2022 during sampling efforts. As a large proportion of released fish were not tagged in 2021, we cannot distinguish ‘wild’ from untagged hatchery-origin individuals.

Table 4. MtDNA haplotype frequencies for the middle Rio Grande population and fish reared from captive spawning. Values from the 2022 monitoring year are shaded for emphasis.

	A	C	D	E	F	I	J	K	M	O	P	Q	S	T	V
1987	45.95	16.22	16.22	5.41	8.11	-	-	2.70	5.41	-	-	-	-	-	-
1999	75.00	-	11.36	6.82	4.55	-	-	2.27	-	-	-	-	-	-	-
2000	76.98	0.79	4.76	4.76	11.90	-	-	0.79	-	-	-	-	-	-	-
2001	57.43	10.89	4.95	3.96	9.90	0.99	0.99	8.91	0.99	0.99	-	-	-	-	-
2002	55.56	19.90	13.70	1.03	5.94	-	0.26	3.36	-	0.26	-	-	-	-	-
2003	67.07	5.39	14.97	2.99	5.39	-	0.60	1.20	0.60	1.80	-	-	-	-	-
2004	59.63	8.70	10.56	1.86	7.45	1.24	-	4.97	1.86	3.11	0.62	-	-	-	-
2005	59.69	12.76	8.93	2.81	8.42	1.53	0.26	1.79	2.81	1.02	-	-	-	-	-
2006	58.58	13.72	9.23	4.75	4.75	0.26	-	4.75	2.90	0.79	-	-	-	0.26	-
2007	62.84	11.01	8.26	2.29	8.72	0.46	-	3.67	0.46	1.83	-	0.46	-	-	-
2008	63.46	11.97	7.91	2.56	6.62	0.64	-	4.49	0.85	0.64	0.21	-	0.64	-	-
2009	61.57	14.01	7.64	2.76	6.37	0.64	0.42	3.40	1.70	1.06	0.21	-	0.21	-	-
2010	57.11	12.09	9.72	3.08	7.11	1.42	-	5.45	1.66	2.37	-	-	-	-	-
2011	57.38	14.21	10.86	2.79	6.41	0.56	-	3.06	3.06	1.11	-	0.28	0.28	-	-
2012	54.28	17.32	9.53	3.70	7.59	0.39	0.39	2.92	2.14	1.75	-	-	-	-	-
2015	55.24	12.59	12.59	1.40	9.79	-	-	2.10	2.10	4.20	-	-	-	-	-
2016	40.51	25.32	9.37	1.77	7.09	0.76	-	3.04	3.29	8.86	-	-	-	-	-
2017	55.44	14.93	10.66	1.28	7.04	0.21	-	1.92	2.13	6.18	-	-	-	-	0.21
2018	44.74	16.51	11.72	1.44	9.09	0.72	-	4.07	2.87	7.89	-	-	-	-	0.96
2019	50.76	23.48	3.79	3.03	4.55	-	-	3.03	1.52	9.85	-	-	-	-	-
2020	48.70	19.62	8.27	1.42	7.33	1.65	-	3.55	1.65	6.86	-	-	-	-	0.95
2021	46.25	21.25	12.50	-	5.83	1.25	-	2.08	6.25	4.58	-	-	-	-	-
2022	40.65	20.18	13.95	0.30	3.26	1.48	-	2.97	2.08	13.95	-	-	-	-	-

Table 4 (cont.). MtDNA haplotype frequencies (%) for the middle Rio Grande population and fish reared from captive spawning. Values from 2022 monitoring year are shaded for emphasis. Haplotypes P, Q, T are omitted from this tables of frequencies for captive stocks as they have not been detected in them.

Captive spawned	A	C	D	E	F	I	J	K	M	O	S	V
ABP13-003-04 WC	40	24	12	-	16	-	-	-	-	8	-	-
ABP16-003 CS	64	25.6	2.6	5.1	-	-	-	-	2.6	-	-	-
Uvalde 2016	38	21	23	-	-	-	-	-	-	14	-	-
16CSDX-003	37	22.2	14.1	3	17.1	-	-	1	-	5.1	-	-
16CSDX-004	37.8	35.7	5.1	-	-	-	-	6.1	-	14.3	1	-
16CSDX-005	39	28	24	-	5	3	-	-	-	1	-	-
ABP18	55.3	40.4	4.3	-	-	-	-	-	-	-	-	-
17CSDX-001	40.8	25.5	24.5	-	2	-	-	-	-	7.1	-	-
17CSDX-002	52	17.3	17.2	-	10.2	-	-	-	-	3.1	-	-
17CSDX-003	41.2	18.6	29.1	2	2.9	-	-	-	-	5.9	-	-
17CSDX-004	39.6	20.8	20.2	1	12.5	-	-	-	-	5.2	-	-
18CSDX-001	44.9	20.4	19.9	1.5	4.1	-	-	0.5	-	8.7	-	-
ABP18-CS	67.3	10.2	0.2	0.2	0.2	-	-	-	4.1	8	-	-
ABP16-001-004	60	24	2	-	8	-	-	-	4	2	-	-
ABP19-CS	57.1	18.4	6.1	-	2	-	-	8.2	-	8.2	-	-
DX-YC19	43.2	15.8	17.8	-	2.7	-	-	-	2.1	18.5	-	-
Los Lunas released	42	14	32	-	4	-	-	-	3	5	-	-
2021 caplot SNARRC	53.5	18.8	14.9	-	5	1	-	1	1	5	-	-
2021 4WIF1 LLSMR	50.5	14.1	7.1	-	4	-	6.1	-	13.1	-	-	5.1
2021 caplot ABP	43.8	39.6	4.2	-	10.4	-	-	-	-	2.1	-	-
2022 caplot SNARRC	31	34	9	-	3	-	-	1	-	22	-	-
2022 caplot LLSMR	51.5	23.2	4	-	12.1		-	6.1	1	2	-	-
2022 caplot ABP	52	28	14	-	-	2	-	-	-	4	-	-

Table 5. MtDNA haplotype frequencies (%) for broodstock held at ABQ BioPark, Southwestern ARRC and the LLSMR. Samples collected for the 2022 monitoring year are shaded for emphasis. Haplotypes P, S, T are omitted from this table of frequencies for captive stocks as they have not been detected in them.

Broodstock	A	C	D	E	F	I	K	M	O	Q	V
ABQ Biopark-Bs-2017	50	26.3	10.9	-	2.7	-	-	-	9.1	-	-
SNARRC- Bs-2017	44.1	22	15.2	3.4	5.1	-	-	-	6.8	-	-
ABQ Biopark-Bs-2018	47.1	26	6.7	0.96	6.7	-	-	3.9	8.7	-	-
SNARRC- Bs-2018	49.4	17.1	13.6	1.2	6.8	1.5	0.9	0.6	8.3	-	0.6
ABQ Biopark-Bs-2019	53	14.2	15.3	-	4.9	0.6	3.3	3.3	5.5	-	-
SNARRC- Bs-2019	47.6	17.1	18.2	1.1	4.8	-	2.7	0.5	7.5	-	0.5
Los Lunas- Bs-2019	47.9	14.8	13.6	-	3.6	0.6	2.4	0.6	16.6	-	-
ABQ Biopark-Bs-2015	68.1	19.2	6.4	-	2.1	-	-	-	4.3	-	-
ABQ Biopark-Bs-2018	43.4	34.3	8.1	3	6.1	-	-	1	4	-	-
SNARRC- Bs-YC2017	53.1	18.4	14.3	2	4.1	1	1	-	6.1	-	-
SNARRC- Bs-YC2018	48	22.5	8.2	1	6.1	5.1	5.1	4.1	-	-	-
SNARRC- Bs-YC2019	54.2	21.9	4.2	1	11.5	1	3.1	1	2.1	-	-
Los Lunas-Bs-ABP18-4WI	41.9	25.7	12.5	0.7	9.6	0.7	2.2	2.2	4.4	-	0.7
2021 ABQ BioPark-Bs-YC16	51	25.5	5.1	2	7.1	-	4.1	2	3.1	-	-
2021 ABQ BioPark-Bs-YC19	46.2	20.6	12.6	1	6	2	3	1.5	6.5	-	0.5
2021 ABQ BioPark-Bs-YC20	42.2	30.6	10.9	-	6.2	0.8	1.2	0.8	6.6	0.4	0.4
2021 SNARRC-Bs-YC20	40.7	30.2	7.5	0.5	11.6	0.5	2.5	0.5	5	-	1
2021 LLSMR-Bs-YC19	34	26	10	-	10	4	2	4	10	-	-
2021 LLSMR-Bs-YC20	47	24.8	7.4	1.3	5.4	0.7	1.3	4.7	7.4	-	-
ABP19_3Wild-Angostura/ABP19-4Wild-San Acacia/ABP20-5Wild_Isleta	46.2	18.3	15.1	0.0	3.2	2.2	4.3	2.2	8.6	-	-
ABP20-4Wild-SanAcacia	38.3	35.1	6.4	2.1	6.4	-	1.1	2.1	6.4	-	2.1
ABP20-4Wild-SanAcacia	36.8	33.7	14.7	1.1	4.2	-	2.1	-	7.4	-	-
ABP21-2Wild-Angostura	43.0	18.3	17.2	0.0	1.1	3.2	3.2	-	12.9	-	1.1
ABP21-2Wild-SanAcacia	48.4	18.9	14.7	2.1	6.3	1.1	-	1.1	6.3	-	1.1
ABP21-3Wild-Isleta	40.4	19.1	14.9	0.0	10.6	-	3.2	-	10.6	-	1.1
2022-SNARRC-BSYC19	34.4	27.8	14.4	2.2	5.6	2.2	2.2	1.1	10.0	-	-
2022-SNARRC-BSYC20	53.5	15.1	11.6	1.2	8.1	1.2	-	3.5	5.8	-	-
2022-LL-BSWC20	37.0	26.1	15.2	1.1	5.4	1.1	-	1.1	13.0	-	-
2022-LL-BSWC21	39.8	26.9	11.8	2.2	6.5	1.1	4.3	3.2	4.3	-	-